Hyperonic equation of state for neutron stars at finite temperature

Supported by:

Hristijan Kochankovski
Àngels Ramos
Laura Tolos

HYP2022
Prague, Czech Republic

30.06.2022

Outline

- Why we need a finite temperature hyperonic Equation of State (EoS)?
- Brief introduction to the FSU2H* model.
- Equation of State (EoS) and composition of hyperonic matter at a constant charge fraction.
- A simple application: $M(R)$ curves for neutron stars at finite temperature.
- Summary

Why we need a finite temperature hyperonic Equation of State (EOS)? (I)

F. Weber, Prog.Part.Nucl.Phys.54:193-288,2005

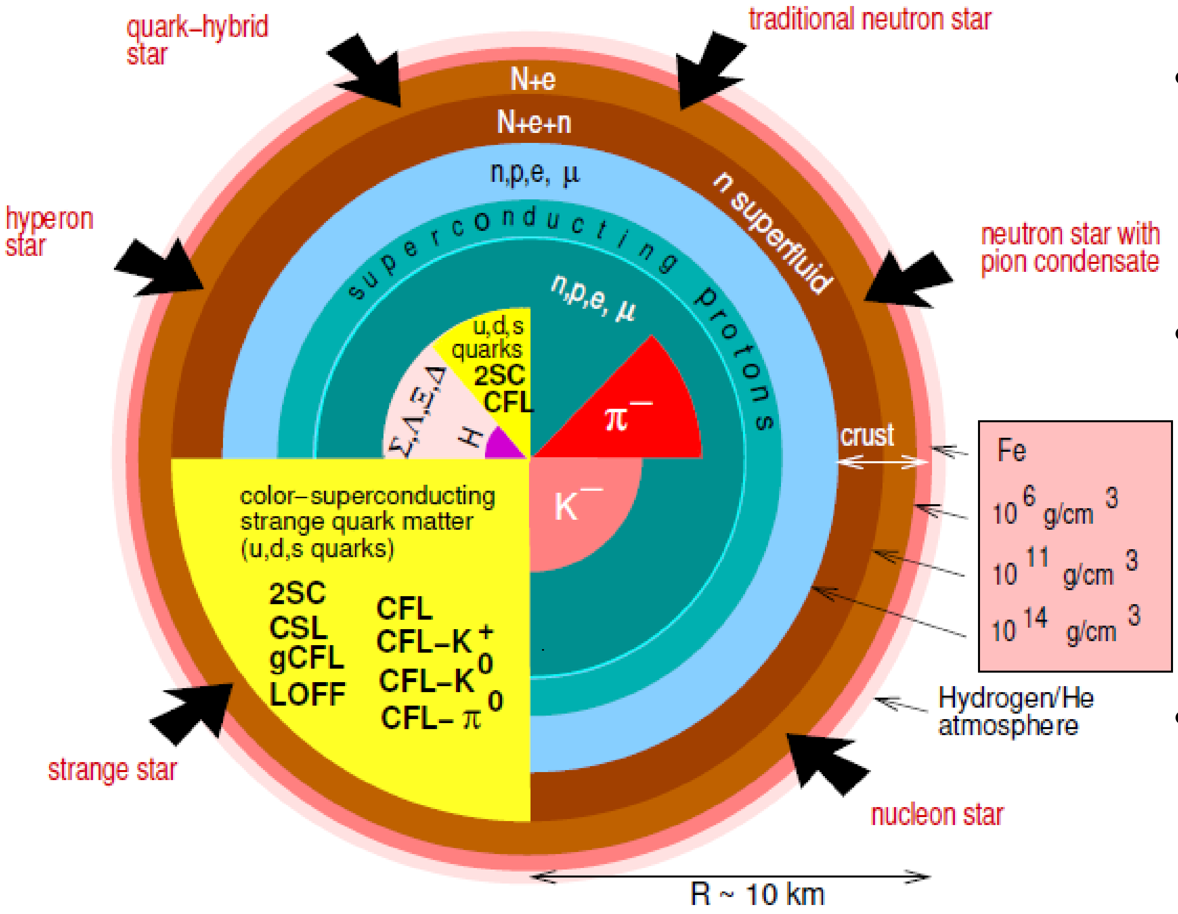

- Hyperons are one type of exotic particles that can appear in the inner core of the neutron star.

- Hyperonic models are still not very well constrained
(large parameter space due to uncertainties in the effective interactions at high densities).

- The finite temperature EoS is a necessary tool to understand the phenomena of core collapse supernovae and neutron star binary mergers.

Why we need a finite temperature hyperonic Equation of State (EOS)? (II)

- The pressure and the energy density at a fixed point in the star, at finite temperature can be decomposed as:

$$P(T) = P_0 + P_{ther}(T)$$
$$\epsilon(T) = \epsilon_0 + \epsilon_{ther}(T)$$

- The relation between $P_{ther}(T)$ and $\epsilon_{ther}(T)$ can be written as:

$$\boldsymbol{P_{ther}(\epsilon_{ther}) = (\Gamma - 1)\epsilon_{ther}}$$

- If one assumes that the thermal index Γ is constant, one can obtain finite temperature EoS just by knowing $T = 0$ EoS.
- However, this approach can be inaccurate, as we showed in:

arXiv:2206.11266

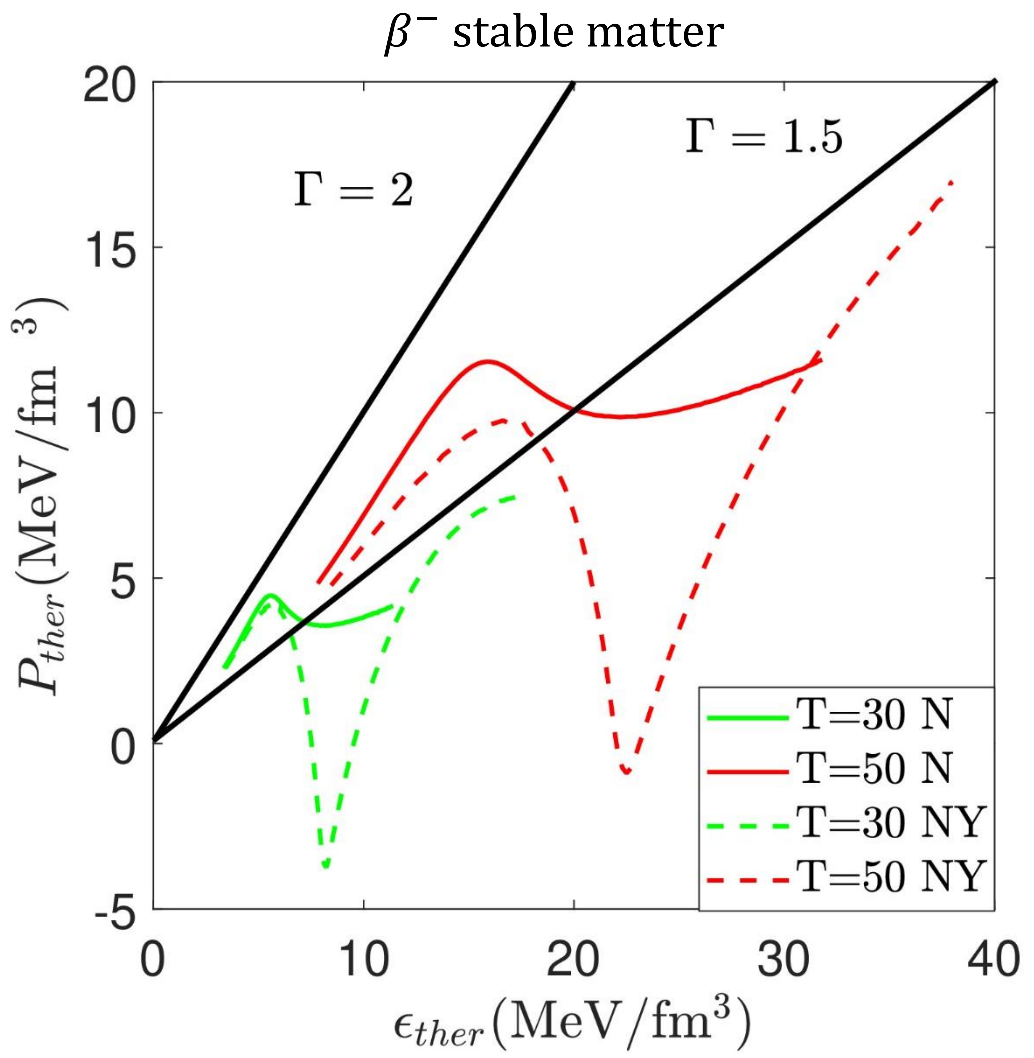

Brief introduction to FSU2H* model

Brief introduction to FSU2H* model

- Belongs to the broad group of relativistic – mean field approaches:

$$
\begin{aligned}
\mathcal{L} &= \sum_b \mathcal{L}_b + \mathcal{L}_m \\
\mathcal{L}_b &= \bar{\Psi}_b(i\gamma_\mu\partial^\mu - q_b\gamma_\mu A^\mu - m_b \\
&\quad + g_{\sigma b}\sigma + g_{\sigma^* b}\sigma^* - g_{\omega b}\gamma_\mu\omega^\mu - g_{\phi b}\gamma_\mu\phi^\mu - g_{\rho,b}\gamma_\mu\vec{I}_b\vec{\rho}^\mu)\Psi_b, \\
\mathcal{L}_m &= \frac{1}{2}\partial_\mu\sigma\partial^\mu\sigma - \frac{1}{2}m_\sigma^2\sigma^2 - \frac{\kappa}{3!}(g_{\sigma b}\sigma)^3 - \frac{\lambda}{4!}(g_{\sigma b})^4 \\
&\quad + \frac{1}{2}\partial_\mu\sigma^*\partial^\mu\sigma^* - \frac{1}{2}m_{\sigma^*}^2\sigma^{*2} \\
&\quad - \frac{1}{4}\Omega^{\mu\nu}\Omega_{\mu\nu} + \frac{1}{2}m_\omega^2\omega_\mu\omega^\mu + \frac{\zeta}{4!}g_{\omega b}^4(\omega_\mu\omega^\mu)^2 \\
&\quad - \frac{1}{4}\vec{R}^{\mu\nu}\vec{R}_{\mu\nu} + \frac{1}{2}m_\rho^2\vec{\rho}_\mu\vec{\rho}^\mu + \Lambda_\omega g_{\rho b}^2\vec{\rho}_\mu\vec{\rho}^\mu g_{\omega b}^2\omega_\mu\omega^\mu \\
&\quad - \frac{1}{4}P^{\mu\nu}P_{\mu\nu} + \frac{1}{2}m_\phi^2\phi_\mu\phi^\mu - \frac{1}{4}F^{\mu\nu}F_{\mu\nu},
\end{aligned}
$$

Brief introduction to FSU2H* model

- Belongs to the broad group of relativistic – mean field approaches:

$$
\begin{aligned}
\mathcal{L} &= \sum_b \mathcal{L}_b + \mathcal{L}_m \\
\mathcal{L}_b &= \bar{\Psi}_b(i\gamma_\mu\partial^\mu - q_b\gamma_\mu A^\mu - m_b \\
&\quad + g_{\sigma b}\sigma + g_{\sigma^* b}\sigma^* - g_{\omega b}\gamma_\mu\omega^\mu - g_{\phi b}\gamma_\mu\phi^\mu - g_{\rho,b}\gamma_\mu\vec{I}_b\vec{\rho}^\mu)\Psi_b, \\
\mathcal{L}_m &= \frac{1}{2}\partial_\mu\sigma\partial^\mu\sigma - \frac{1}{2}m_\sigma^2\sigma^2 - \frac{\kappa}{3!}(g_{\sigma b}\sigma)^3 - \frac{\lambda}{4!}(g_{\sigma b})^4 \\
&\quad + \frac{1}{2}\partial_\mu\sigma^*\partial^\mu\sigma^* - \frac{1}{2}m_{\sigma^*}^2\sigma^{*2} \\
&\quad - \frac{1}{4}\Omega^{\mu\nu}\Omega_{\mu\nu} + \frac{1}{2}m_\omega^2\omega_\mu\omega^\mu + \frac{\zeta}{4!}g_{\omega b}^4(\omega_\mu\omega^\mu)^2 \\
&\quad - \frac{1}{4}\vec{R}^{\mu\nu}\vec{R}_{\mu\nu} + \frac{1}{2}m_\rho^2\vec{\rho}_\mu\vec{\rho}^\mu + \Lambda_\omega g_{\rho b}^2\vec{\rho_\mu}\vec{\rho}^\mu g_{\omega b}^2\omega_\mu\omega^\mu \\
&\quad - \frac{1}{4}P^{\mu\nu}P_{\mu\nu} + \frac{1}{2}m_\phi^2\phi_\mu\phi^\mu - \frac{1}{4}F^{\mu\nu}F_{\mu\nu},
\end{aligned}
$$

- Main characteristics of the cold EoS:

- Reproduces experimental results around ρ_0.

ρ_0 (fm^{-3})	E/A (MeV)	K (MeV)	m_N^*/m_N (ρ_0)	$E_{sym}(\rho_0)$ (MeV)	L (MeV)	K_{sym} (MeV)
0.1505	-16.28	238.0	0.593	30.5	44.5	86.4

Brief introduction to FSU2H* model

- Belongs to the broad group of relativistic – mean field approaches:

$$
\begin{aligned}
\mathcal{L} &= \sum_b \mathcal{L}_b + \mathcal{L}_m \\
\mathcal{L}_b &= \bar{\Psi}_b(i\gamma_\mu \partial^\mu - q_b\gamma_\mu A^\mu - m_b \\
&\quad + g_{\sigma b}\sigma + g_{\sigma^* b}\sigma^* - g_{\omega b}\gamma_\mu\omega^\mu - g_{\phi b}\gamma_\mu\phi^\mu - g_{\rho,b}\gamma_\mu \vec{I}_b\vec{\rho}^\mu)\Psi_b, \\
\mathcal{L}_m &= \frac{1}{2}\partial_\mu\sigma\partial^\mu\sigma - \frac{1}{2}m_\sigma^2\sigma^2 - \frac{\kappa}{3!}(g_{\sigma b}\sigma)^3 - \frac{\lambda}{4!}(g_{\sigma b})^4 \\
&\quad + \frac{1}{2}\partial_\mu\sigma^*\partial^\mu\sigma^* - \frac{1}{2}m_{\sigma^*}^2\sigma^{*2} \\
&\quad - \frac{1}{4}\Omega^{\mu\nu}\Omega_{\mu\nu} + \frac{1}{2}m_\omega^2\omega_\mu\omega^\mu + \frac{\zeta}{4!}g_{\omega b}^4(\omega_\mu\omega^\mu)^2 \\
&\quad - \frac{1}{4}\vec{R}^{\mu\nu}\vec{R}_{\mu\nu} + \frac{1}{2}m_\rho^2\vec{\rho}_\mu\vec{\rho}^\mu + \Lambda_\omega g_{\rho b}^2\vec{\rho}_\mu\vec{\rho}^\mu g_{\omega b}^2\omega_\mu\omega^\mu \\
&\quad - \frac{1}{4}P^{\mu\nu}P_{\mu\nu} + \frac{1}{2}m_\phi^2\phi_\mu\phi^\mu - \frac{1}{4}F^{\mu\nu}F_{\mu\nu},
\end{aligned}
$$

- Main characteristics of the cold EoS:

- Reproduces experimental results around ρ_0.

ρ_0 (fm^{-3})	E/A (MeV)	K (MeV)	m_N^*/m_N (ρ_0)	$E_{sym}(\rho_0)$ (MeV)	L (MeV)	K_{sym} (MeV)
0.1505	-16.28	238.0	0.593	30.5	44.5	86.4

- Reproduces astrophysical constraints at high densities.

$M_{\mathbf{max}}$ ($M_\odot$)	$R(M_{\mathbf{max}})$ (km)	$R(1.4M_\odot)$ (km)	$\mathbf{\Lambda}(1.4M_\odot)$
2.03	12.02	13.08	526.3

Equation of State (EoS) and composition of an hyperonic matter at a constant charge fraction (I)

- Contrary to an already evolved neutron star, some processes require baryonic EoS at an arbitrary charge fraction:

$$Y_Q = \sum_Q \frac{\rho_Q}{\rho_B}$$

- Thus, the finite temperature baryonic EoS becomes a function of three parameters: temperature T, baryonic density ρ_B and charge fraction Y_Q.

- For a general use of the EoS, one needs a table of the composition and the thermodynamic properties of the matter at each grid point

Wide range of values to **account for conditions in proto-neutron stars (PNS) and NS mergers:**

T = (0 – 100) MeV

$$\rho_B = (0.5 - 10)\rho_0$$

$$Y_Q = (0 - 0.6)$$

Equation of State (EoS) and composition of an hyperonic matter at a constant charge fraction (II)

Equation of State (EoS) and composition of an hyperonic matter at a constant charge fraction (II)

- Between different baryons a weak interaction equilibrium is assumed:

$$\mu_n = \mu_\Lambda = \mu_{\Sigma^0} = \mu_{\Xi^0}$$
$$\mu_p = \mu_{\Sigma^+}$$
$$\mu_{\Sigma^-} = \mu_{\Xi^-} = 2\mu_n - \mu_p$$

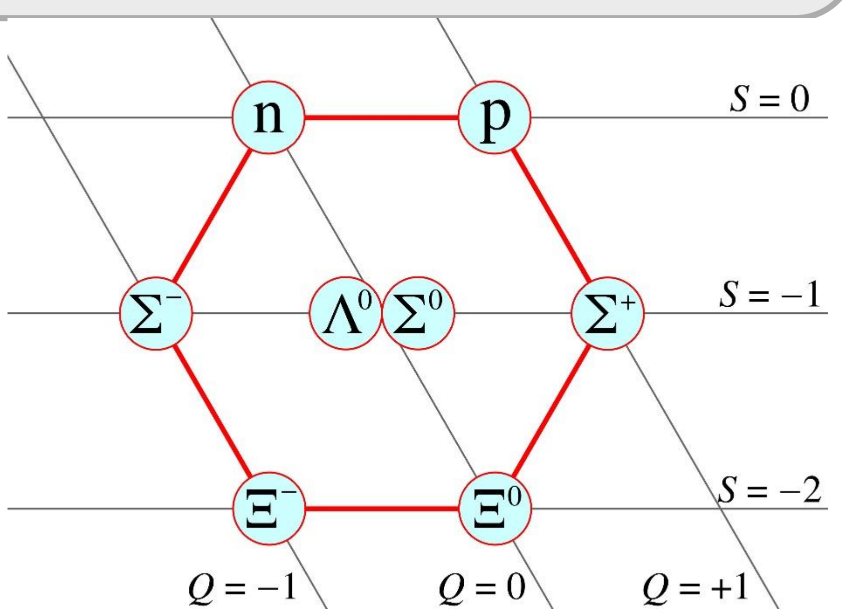

Equation of State (EoS) and composition of an hyperonic matter at a constant charge fraction (II)

- Between different baryons a weak interaction equilibrium is assumed:

$$\mu_n = \mu_\Lambda = \mu_{\Sigma^0} = \mu_{\Xi^0}$$
$$\mu_p = \mu_{\Sigma^+}$$
$$\mu_{\Sigma^-} = \mu_{\Xi^-} = 2\mu_n - \mu_p$$

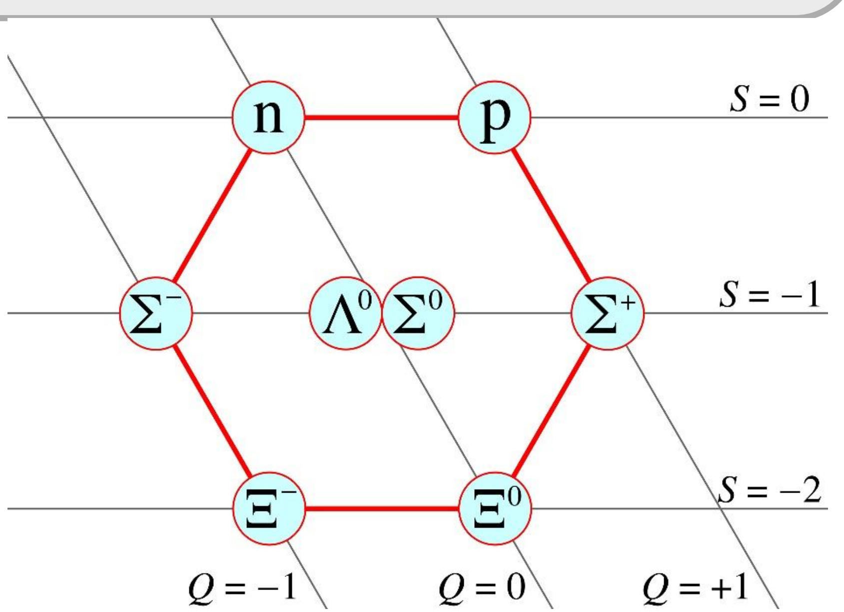

- To inspect the properties of the EoS we show calculations for two temperatures:

$$T = 25 \text{ MeV and } T = 75 \text{ MeV}$$

- and two different charge fractions:

$$Y_q = 0.01 \text{ and } Y_q = 0.5$$

Equation of State (EoS) and composition of an hyperonic matter at a constant charge fraction (II)

- Between different baryons a weak interaction equilibrium is assumed:

$$\mu_n = \mu_\Lambda = \mu_{\Sigma^0} = \mu_{\Xi^0}$$
$$\mu_p = \mu_{\Sigma^+}$$
$$\mu_{\Sigma^-} = \mu_{\Xi^-} = 2\mu_n - \mu_p$$

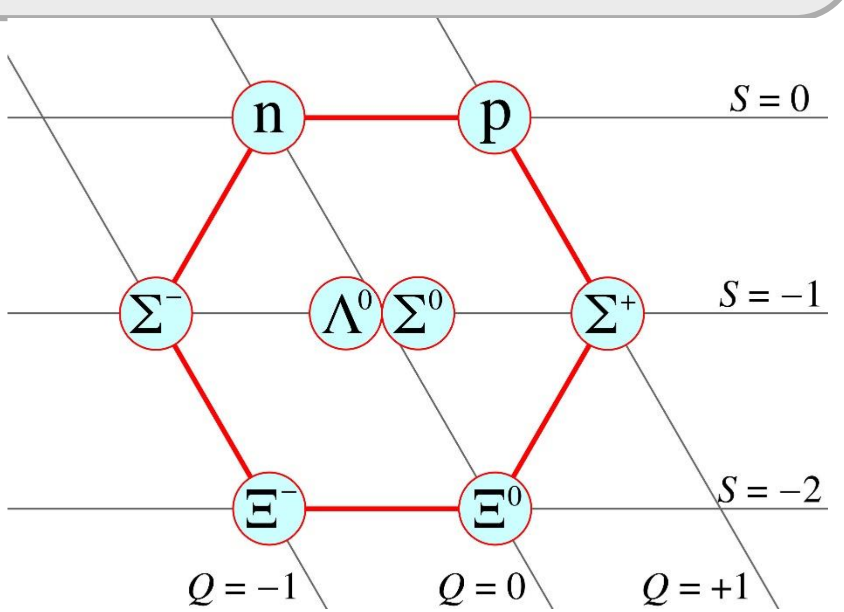

- To inspect the properties of the EoS we show calculations for two temperatures:

$$T = 25 \text{ MeV and } T = 75 \text{ MeV}$$

- and two different charge fractions:

$$Y_q = 0.01 \text{ and } Y_q = 0.5$$

In pure nucleonic matter, the first case would correspond to almost pure neutron matter, while the second one would correspond to symmetric nuclear matter.

Composition of hyperonic matter at fixed Y_Q (I)

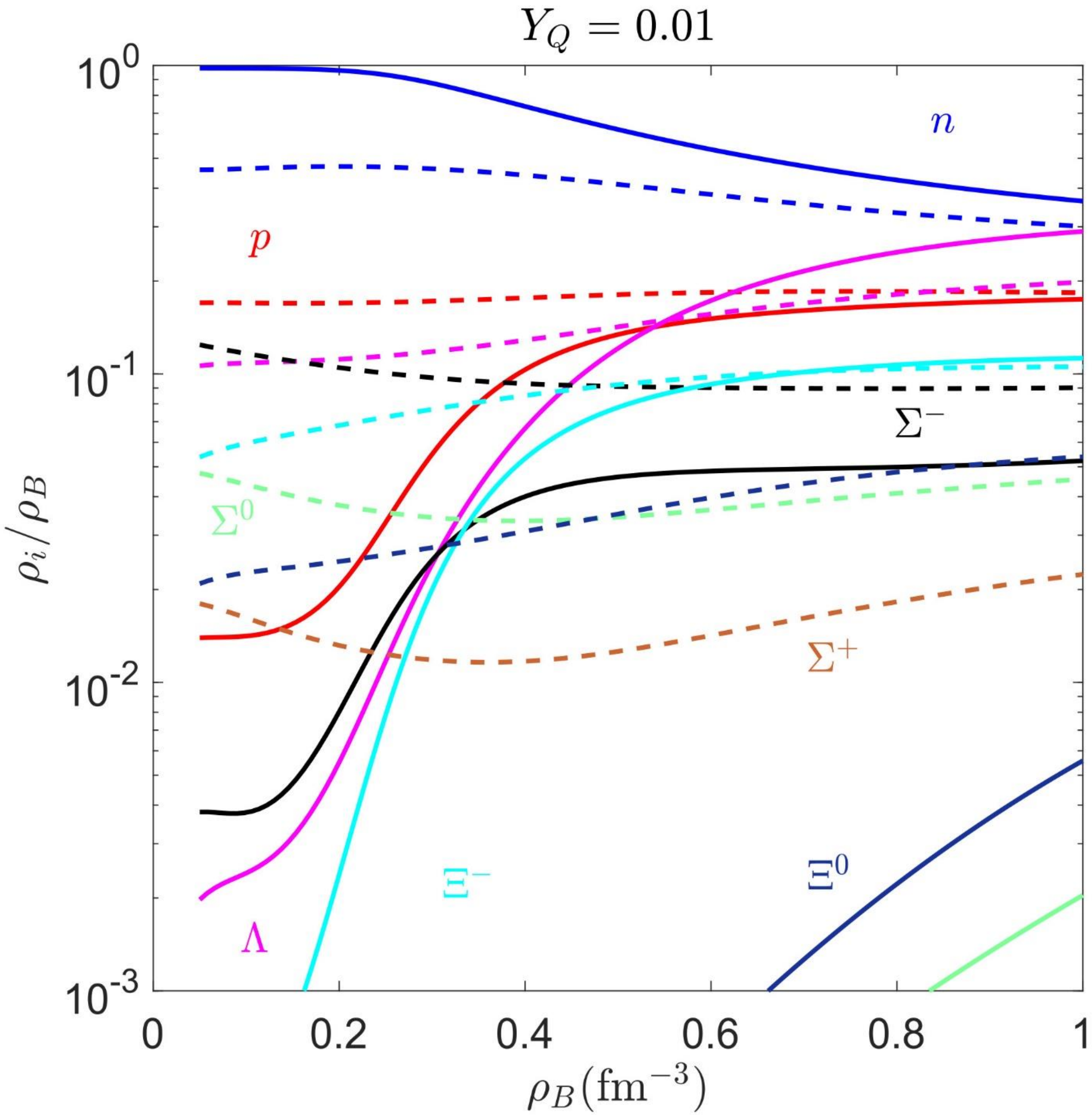

$T = 25$ MeV
$T = 75$ MeV

Composition of hyperonic matter at fixed Y_Q (I)

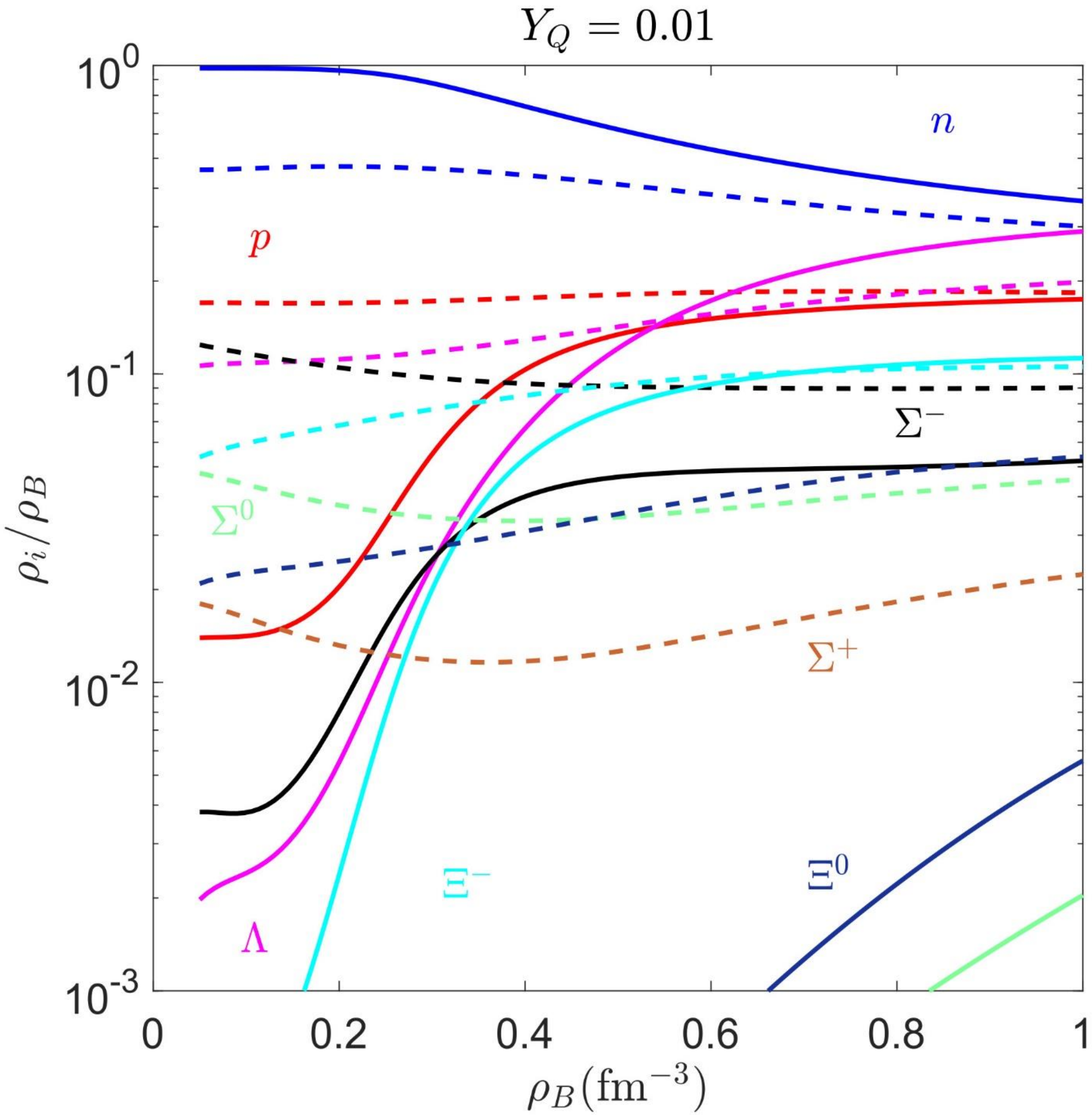

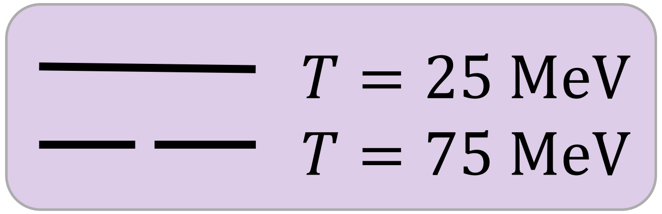

- Hyperons significantly change the composition pattern of matter.

Composition of hyperonic matter at fixed Y_Q (I)

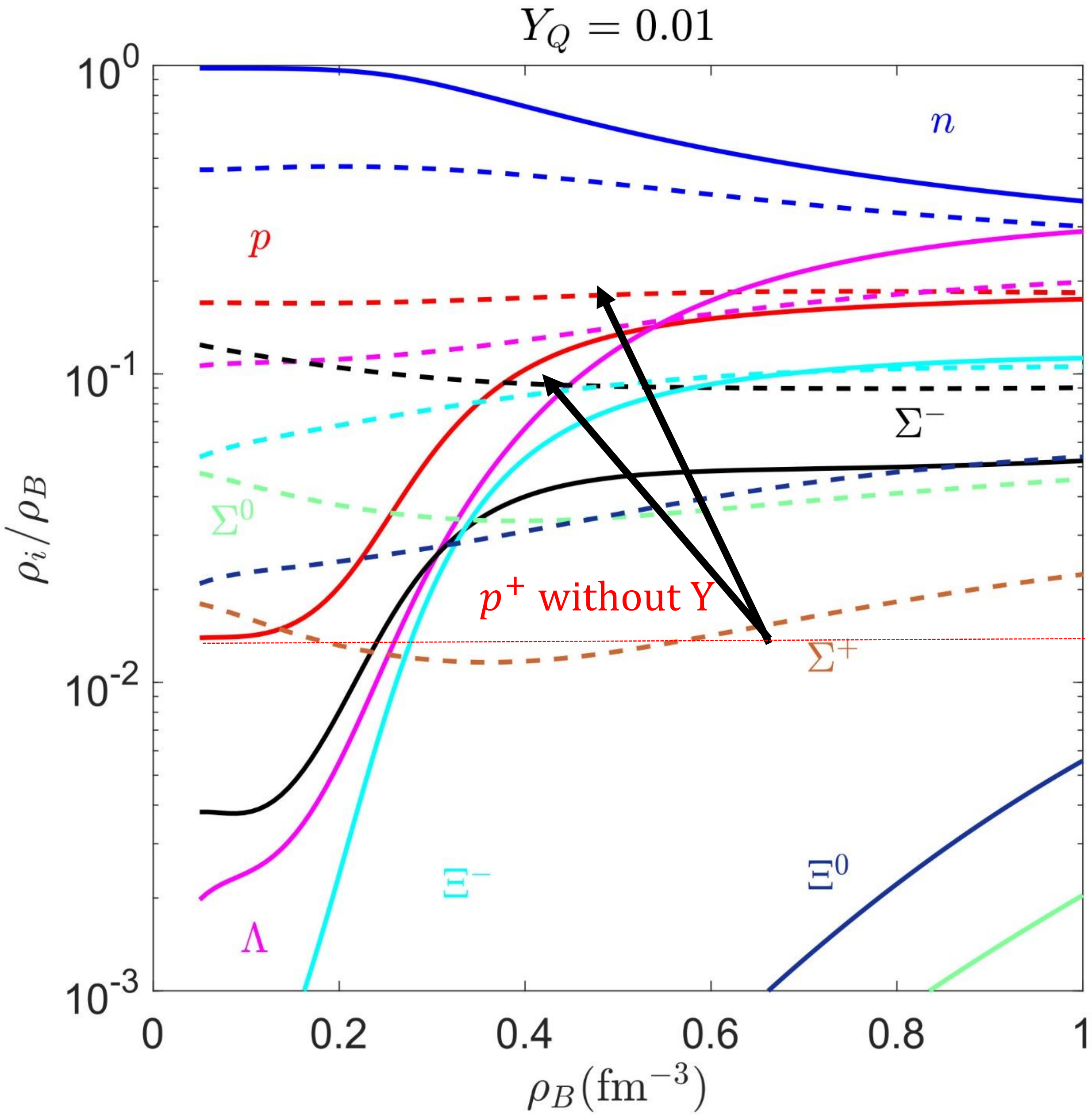

—— $T = 25$ MeV
— — $T = 75$ MeV

- Hyperons significantly change the composition pattern of matter.
- Producing negative charged hyperons allow for protons to be much more abundant than in case without hyperons.

Composition of hyperonic matter at fixed Y_Q (I)

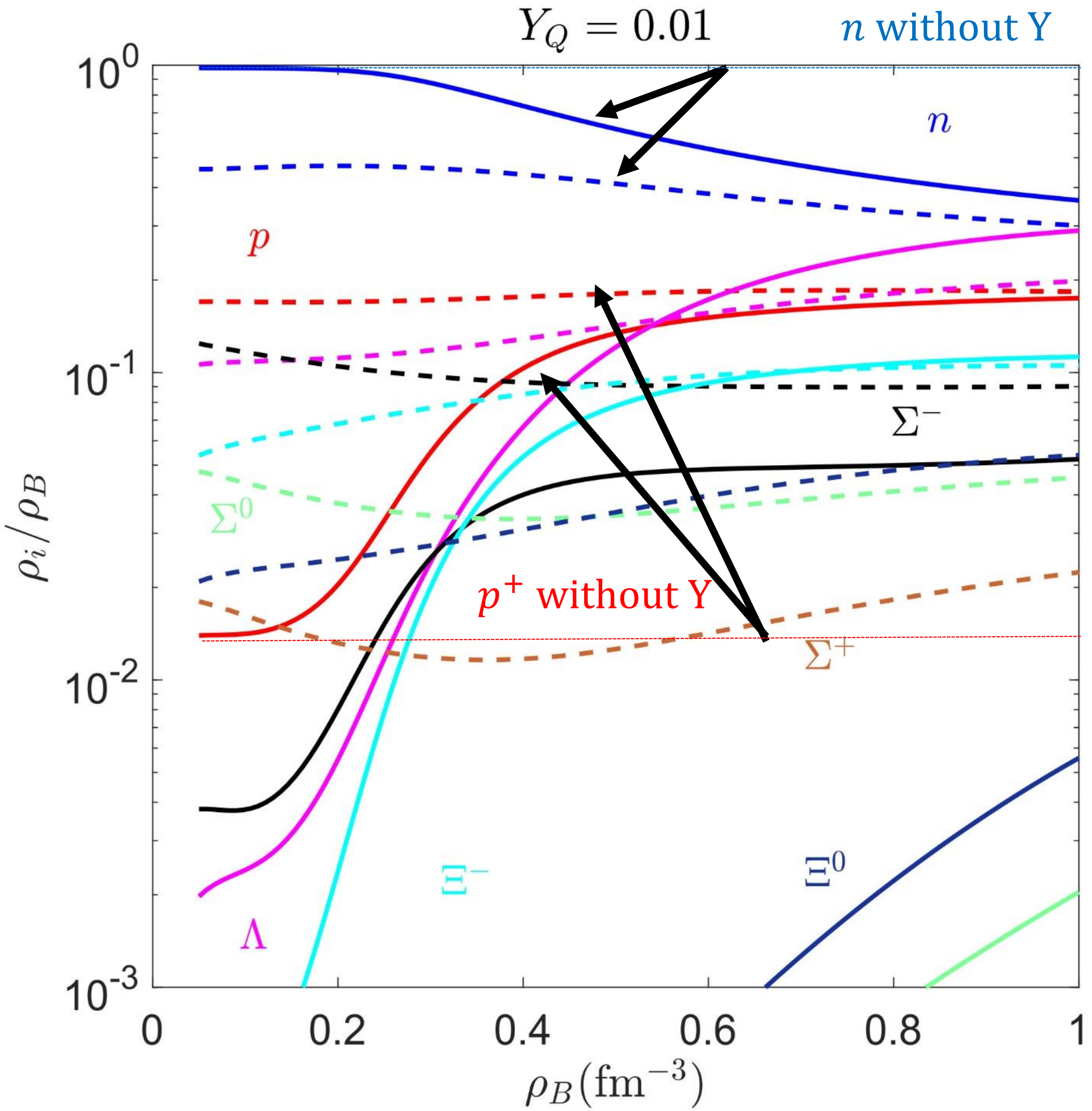

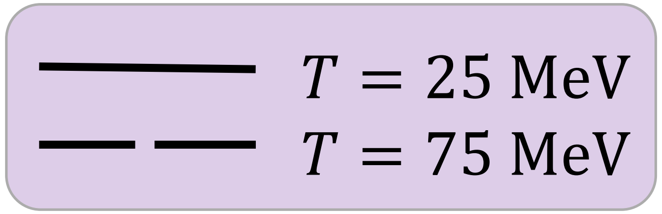

- Hyperons significantly change the composition pattern of matter.
- Producing negative charged hyperons allow for protons to be much more abundant than in case without hyperons.
- On the contrary, neutron abundance is significantly reduced.
- The increase of the temperature has an effect of smoothing out the changes – the composition pattern at high temperatures varies slowly.

Composition of hyperonic matter at fixed Y_Q (II)

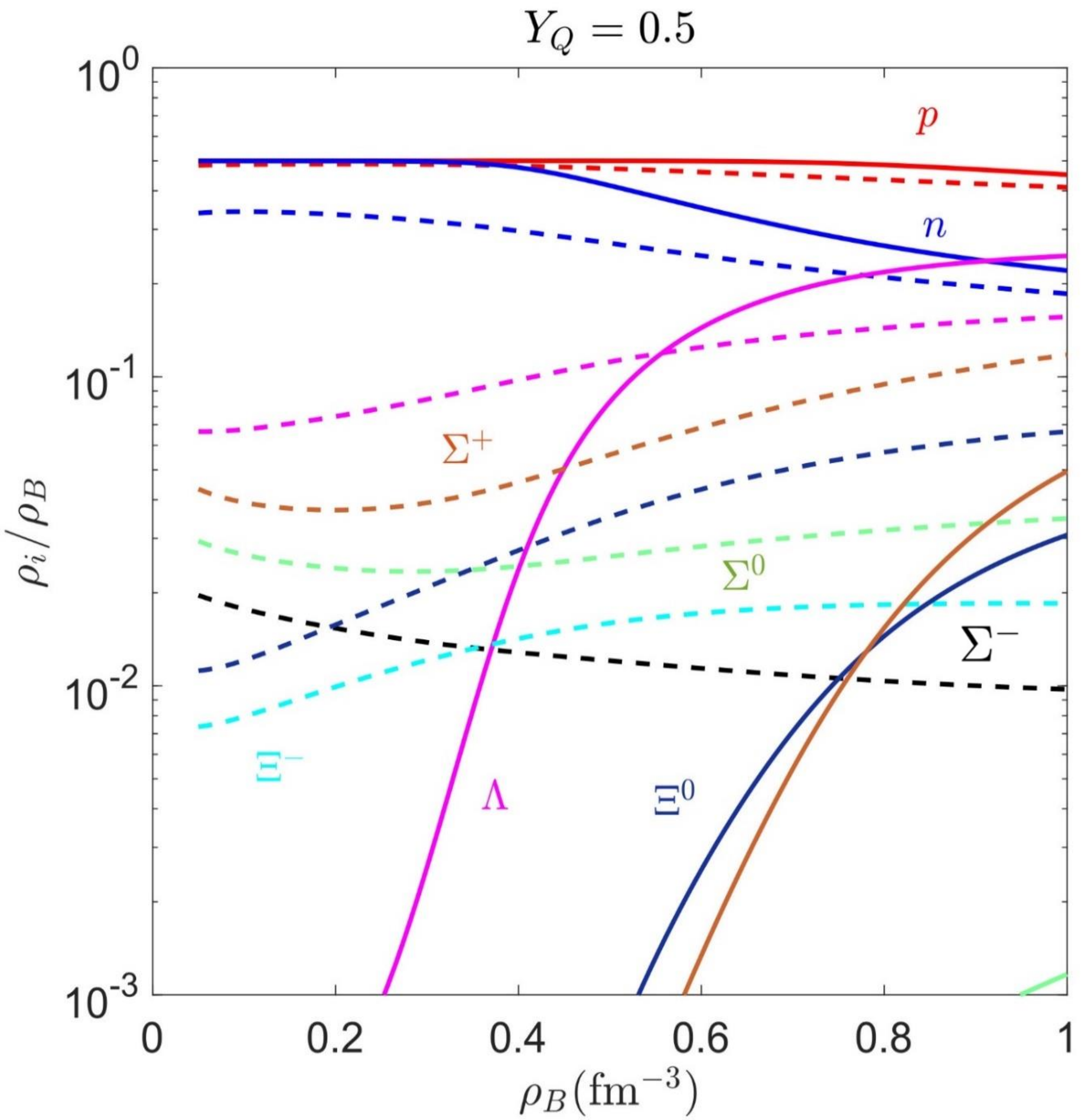

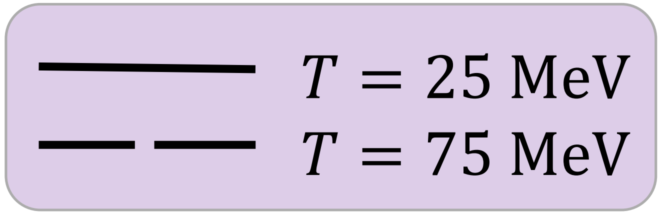

Composition of hyperonic matter at fixed Y_Q (II)

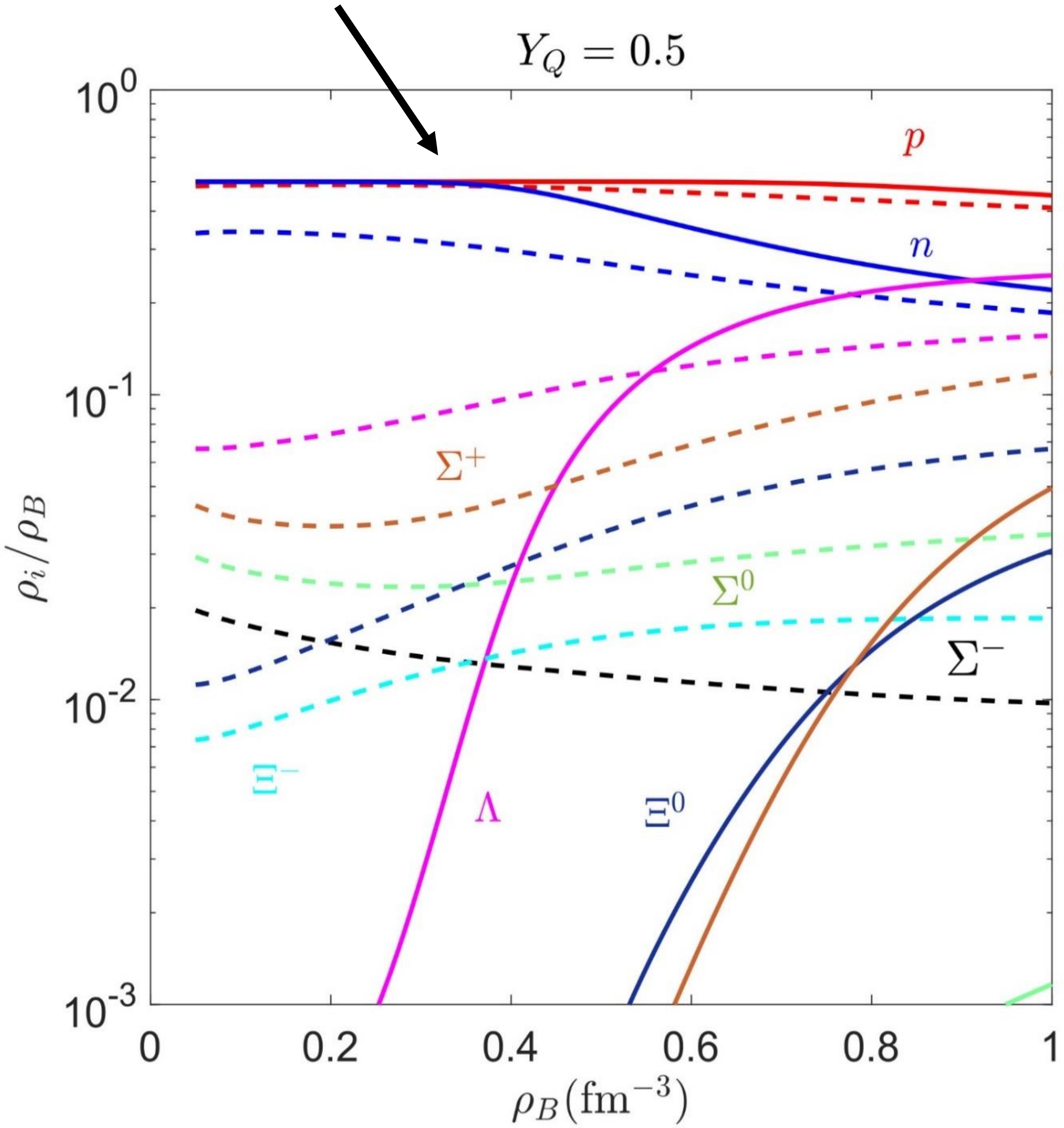

$T = 25$ MeV

$T = 75$ MeV

- At low and moderate temperatures such as $T = 25$ MeV, matter stays isospin symmetric at the beginning of the core.

Composition of hyperonic matter at fixed Y_Q (II)

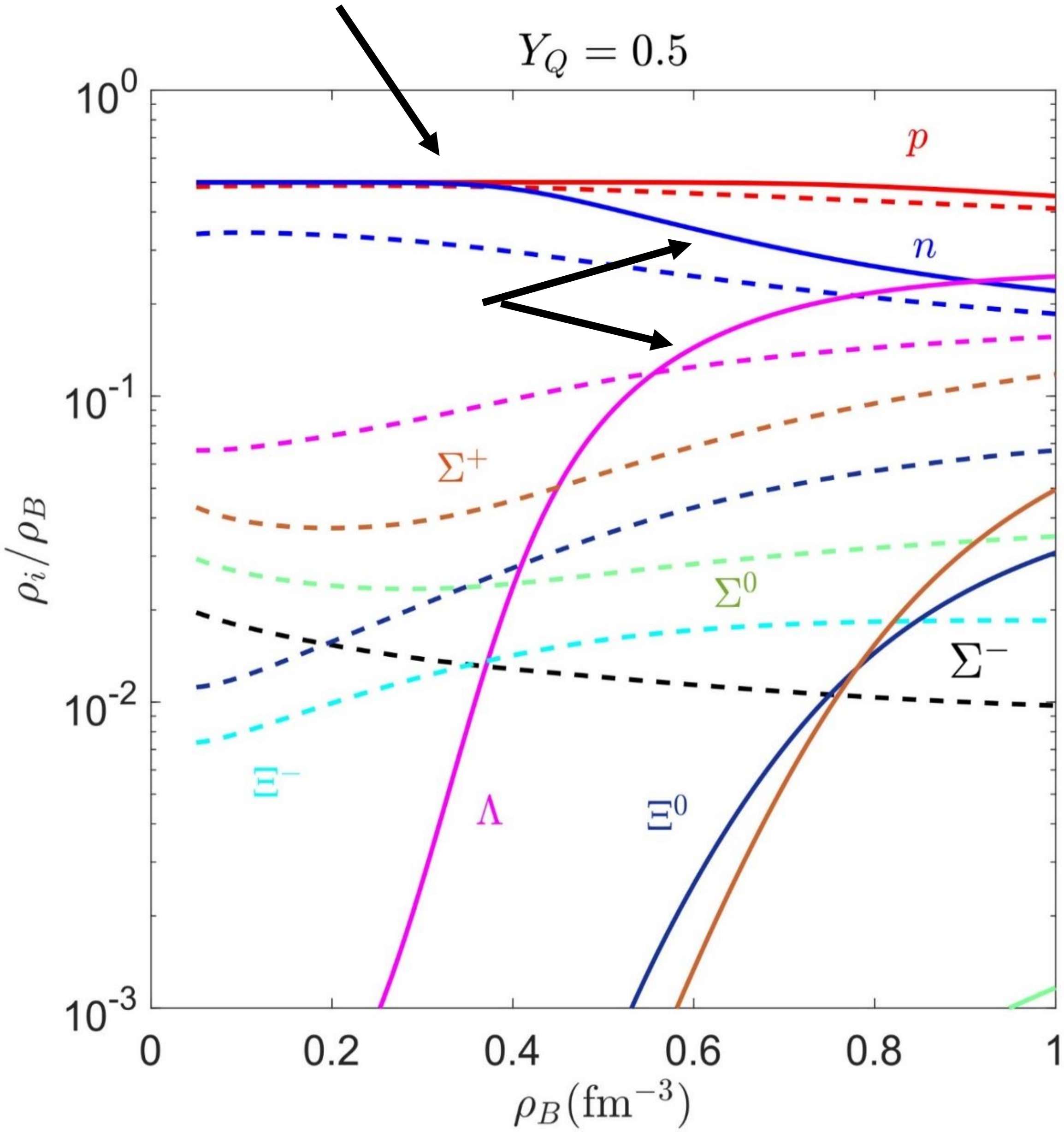

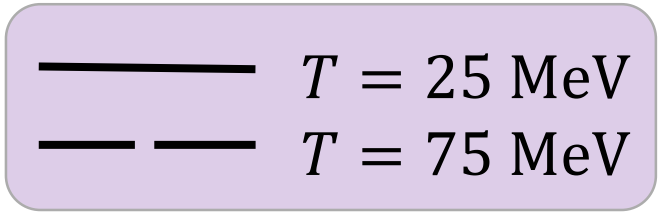

- At low and moderate temperatures such as $T = 25$ MeV, matter stays isospin symmetric at the beginning of the core.
- At higher densities the symmetry is broken and neutrons are quickly converted into Λ hyperons.

Composition of hyperonic matter at fixed Y_Q (II)

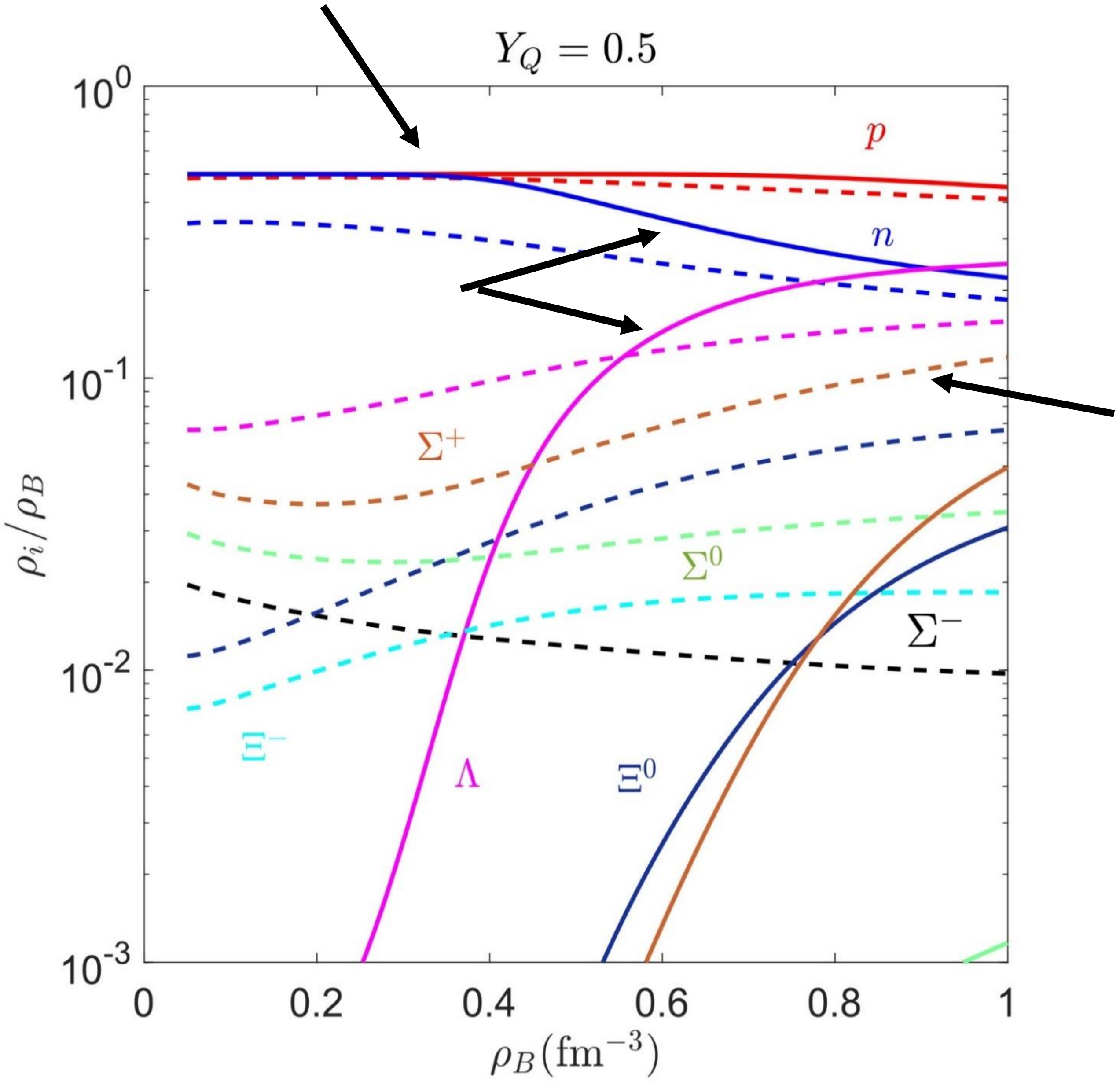

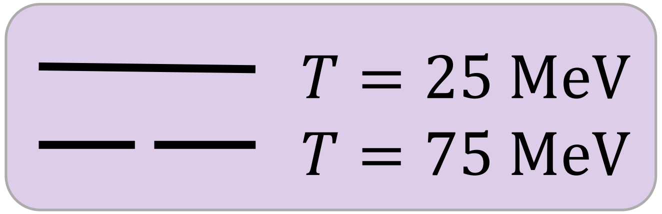

- At low and moderate temperatures such as $T = 25$ MeV, matter stays isospin symmetric at the beginning of the core.

- At higher densities the symmetry is broken and neutrons are quickly converted into Λ hyperons.

- At high temperatures, there is a considerable amount of Σ^+ at any point of the core.

$p(\rho_B)$ and $E/A(\rho_B)$ of hyperonic matter at fixed Y_Q

$p(\rho_B)$ and $E/A(\rho_B)$ of hyperonic matter at fixed Y_Q

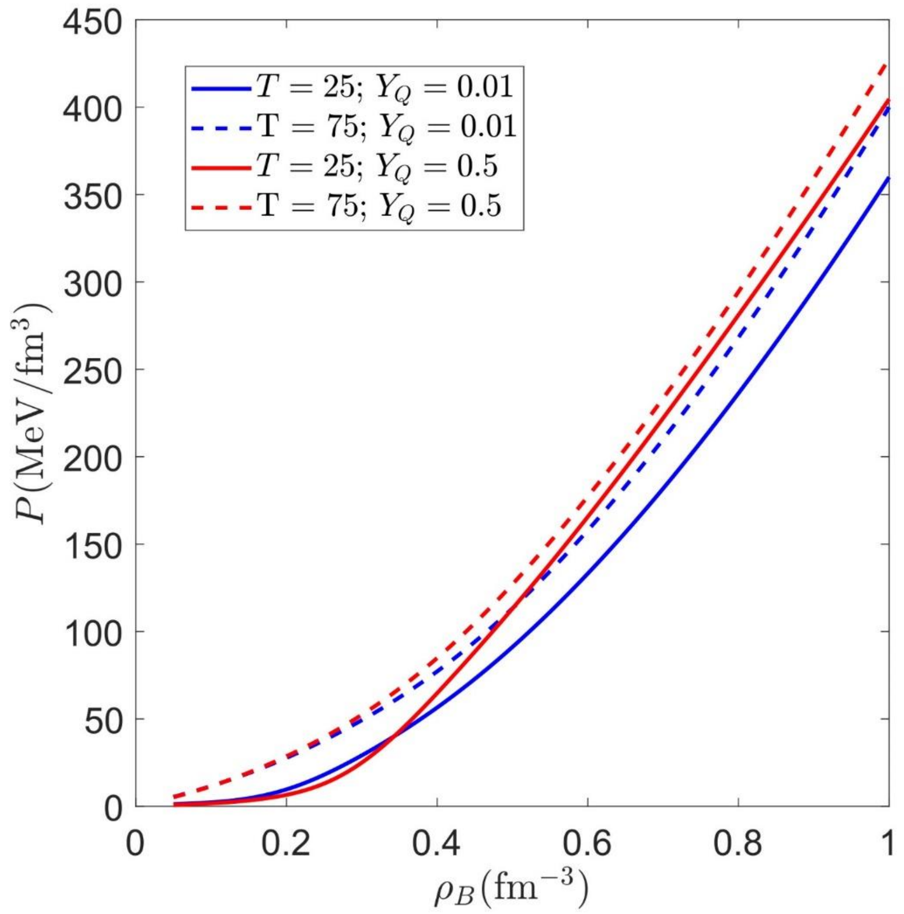

$p(\rho_B)$ and $E/A(\rho_B)$ of hyperonic matter at fixed Y_Q

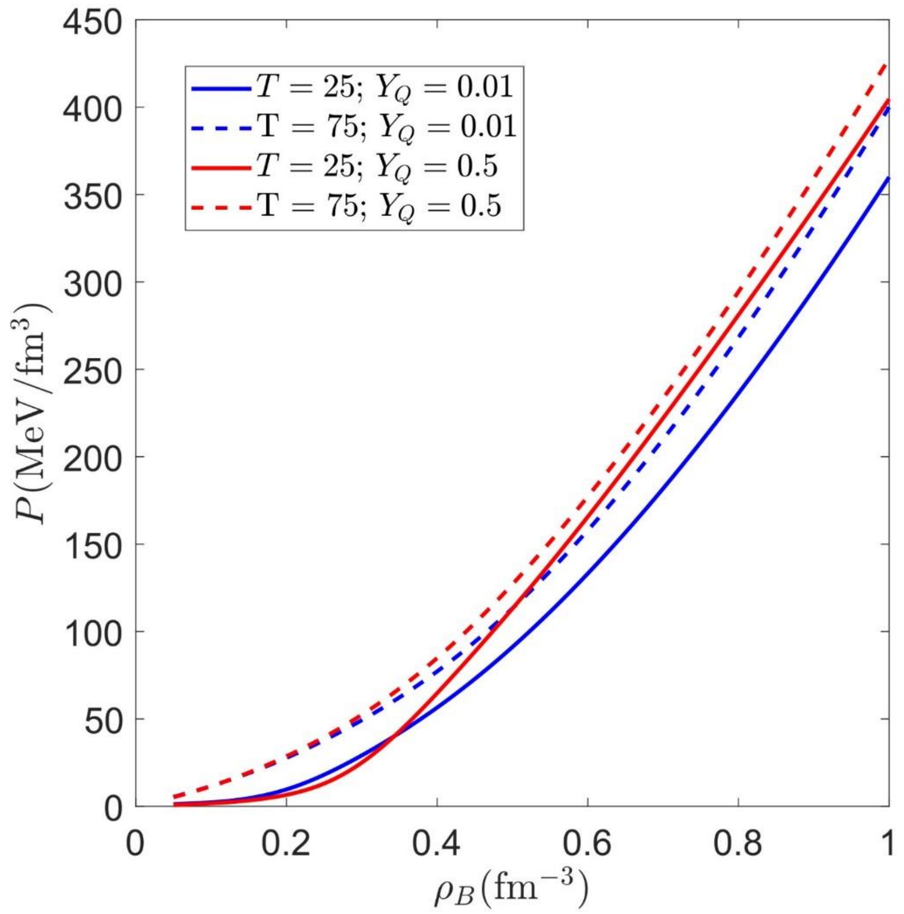

- The pressure strongly depends on T and Y_Q.

$p(\rho_B)$ and $E/A(\rho_B)$ of hyperonic matter at fixed Y_Q

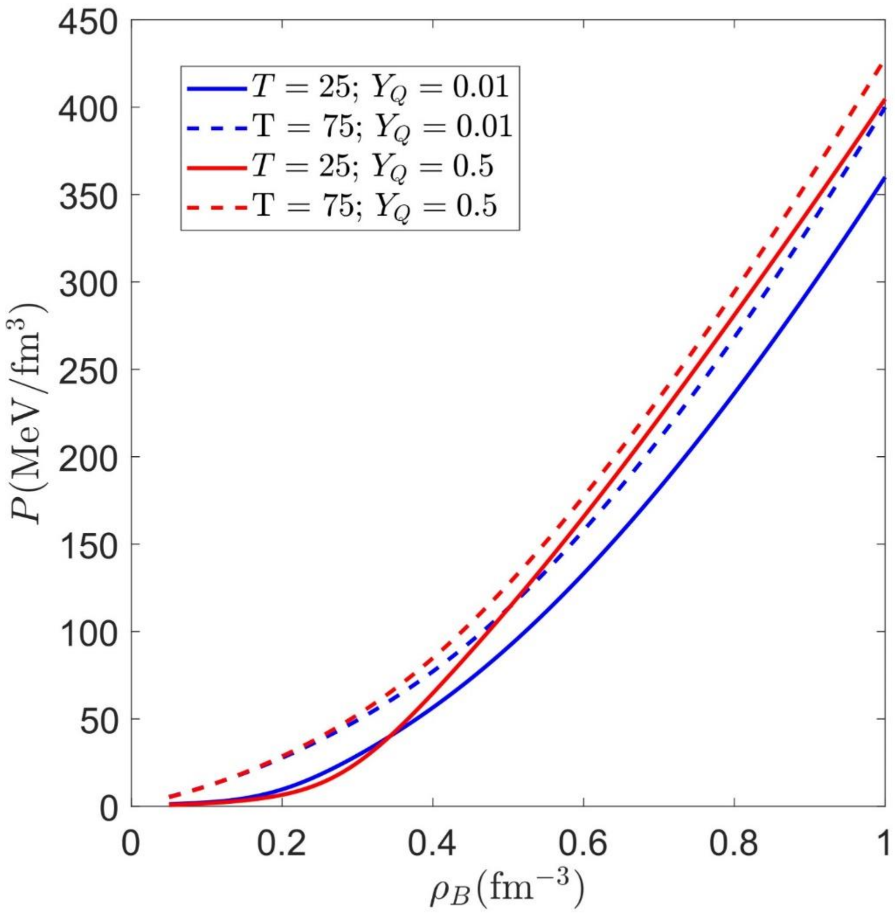

- The pressure strongly depends on T and Y_Q.
- When matter is degenerate (high density), the temperature dependence of the pressure is weaker .

$p(\rho_B)$ and $E/A(\rho_B)$ of hyperonic matter at fixed Y_Q

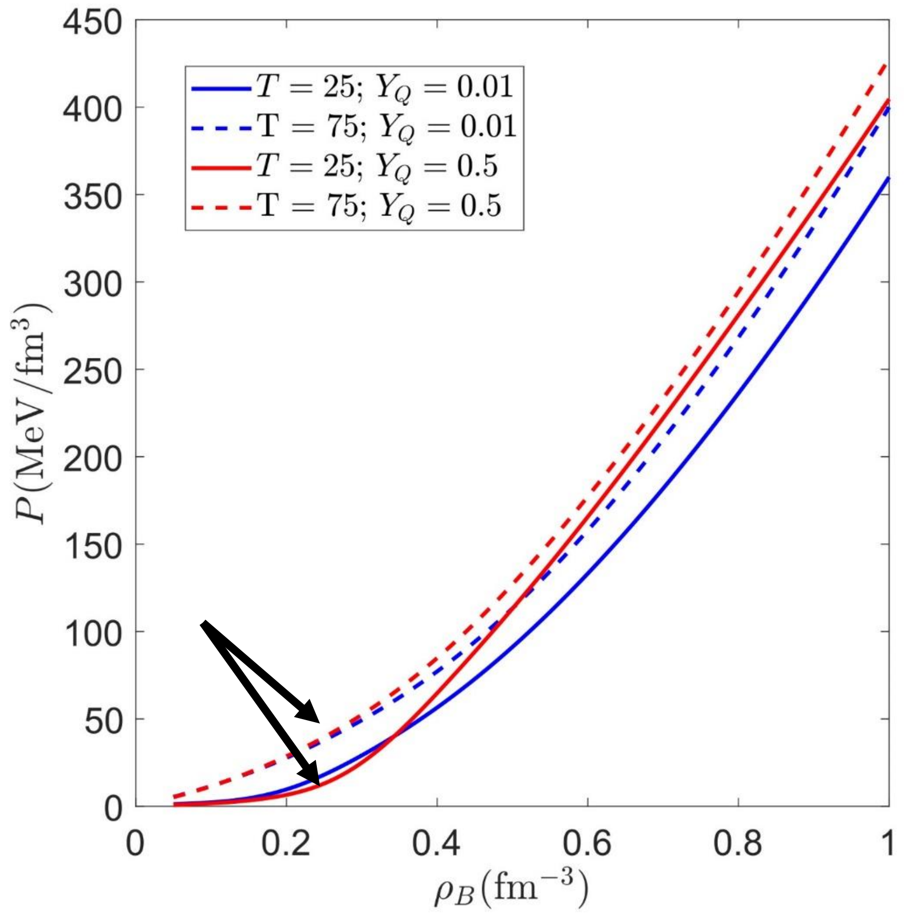

- The pressure strongly depends on T and Y_Q.
- When matter is degenerate (high density), the temperature dependence of the pressure is weaker .

$p(\rho_B)$ and $E/A(\rho_B)$ of hyperonic matter at fixed Y_Q

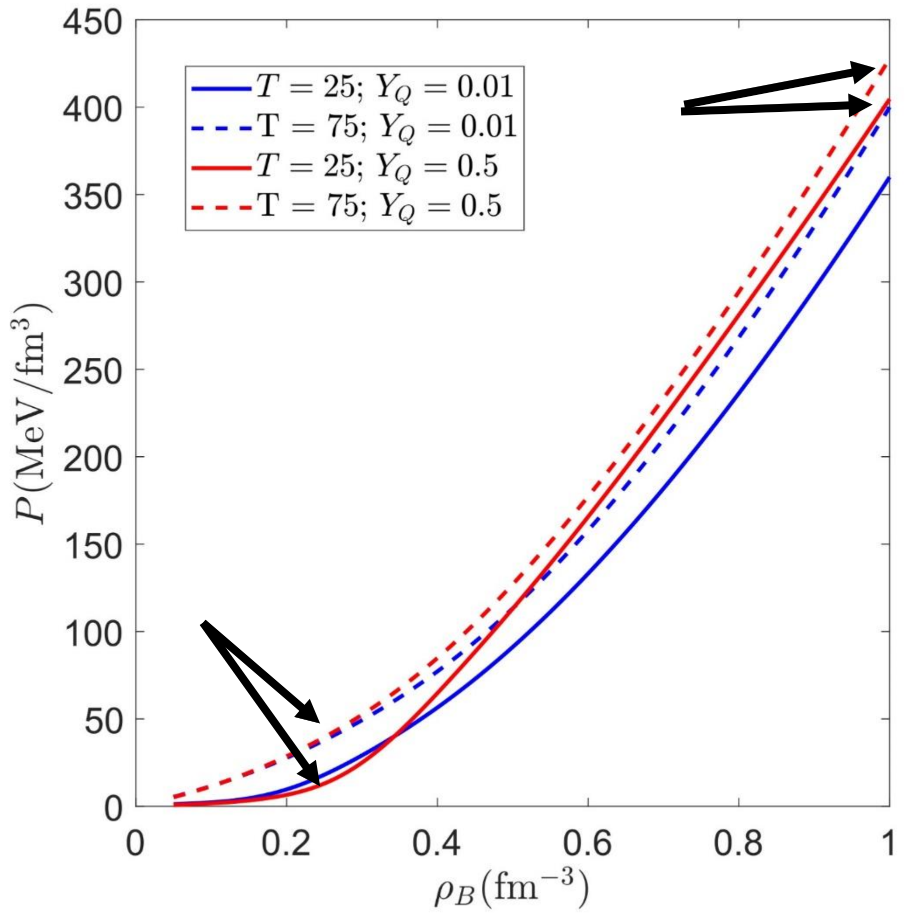

- The pressure strongly depends on T and Y_Q.
- When matter is degenerate (high density), the temperature dependence of the pressure is weaker .

$p(\rho_B)$ and $E/A(\rho_B)$ of hyperonic matter at fixed Y_Q

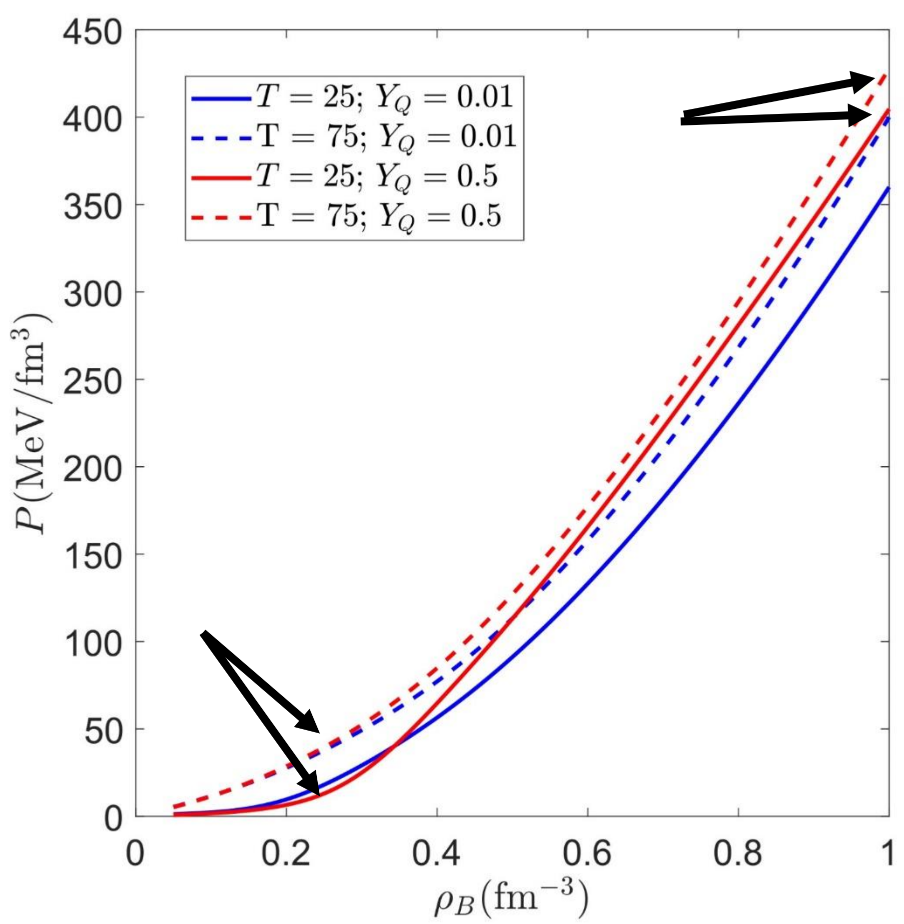

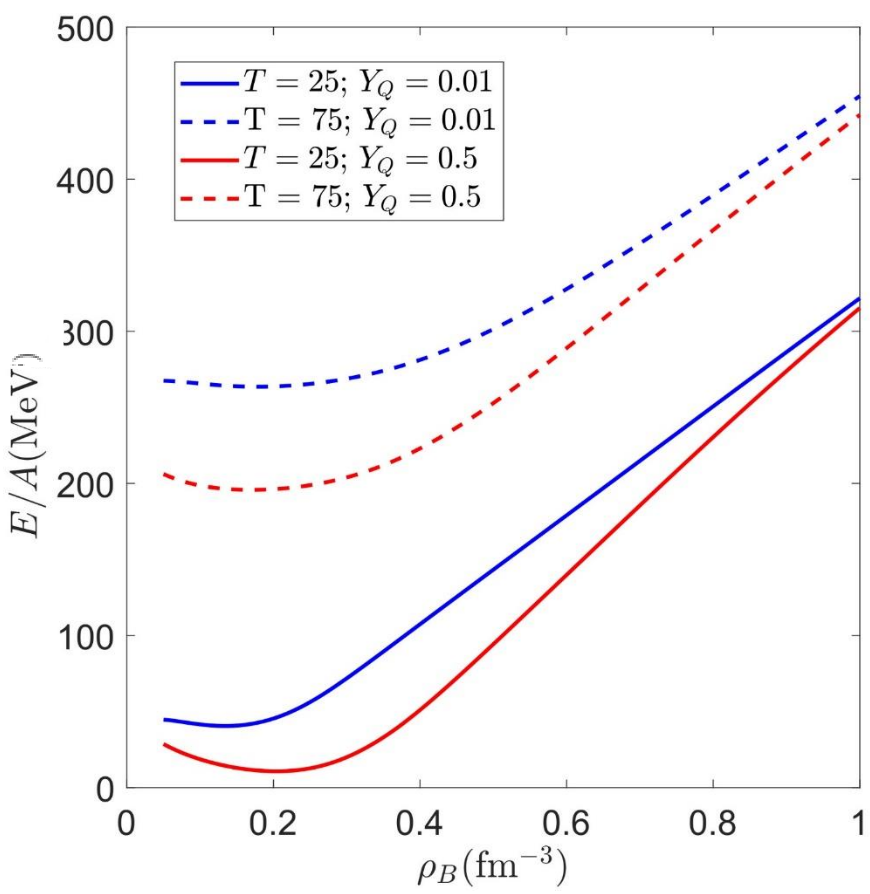

- The pressure strongly depends on T and Y_Q.
- When matter is degenerate (high density), the temperature dependence of the pressure is weaker .

- E/A is larger at higher temperatures.
- E/A weakly depends on Y_Q, at high densities.

Application: $M(R)$ of a β^- stable star

Application: $M(R)$ of a β^- stable star

- One of the strongest constraints that we have is the maximum mass that the model predicts.

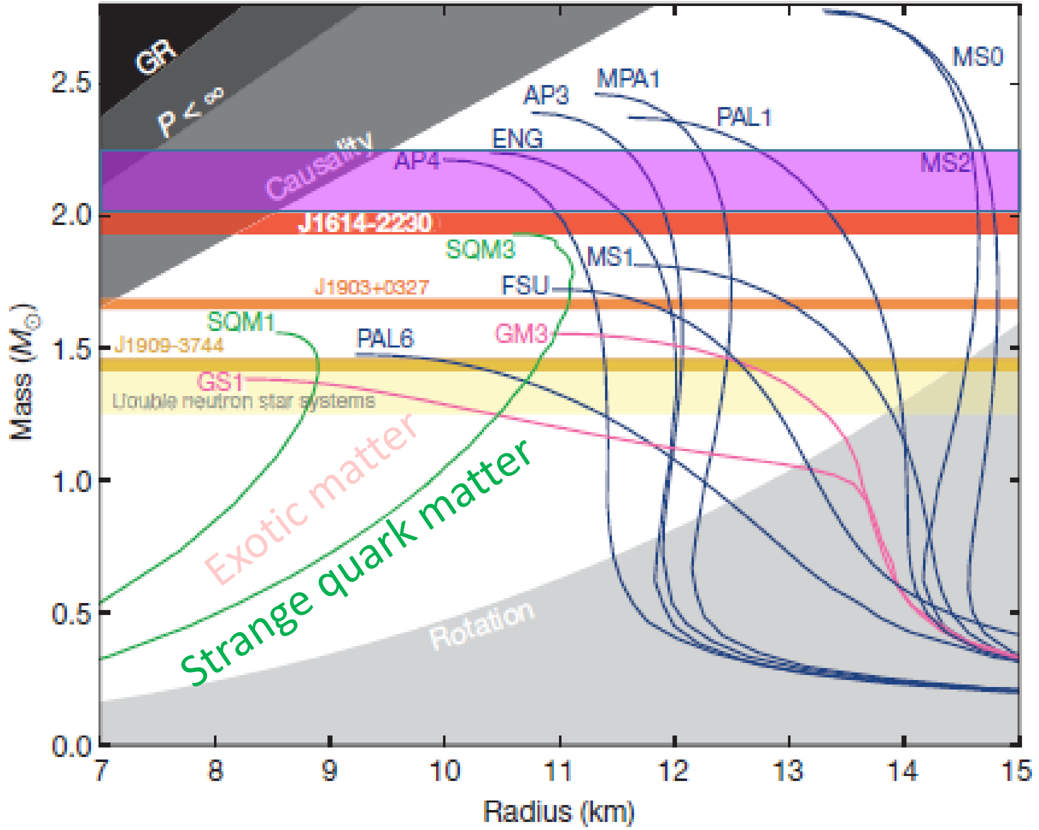

doi:10.1038/nature09466

Application: $M(R)$ of a β^- stable star

- One of the strongest constraints that we have is the maximum mass that the model predicts.

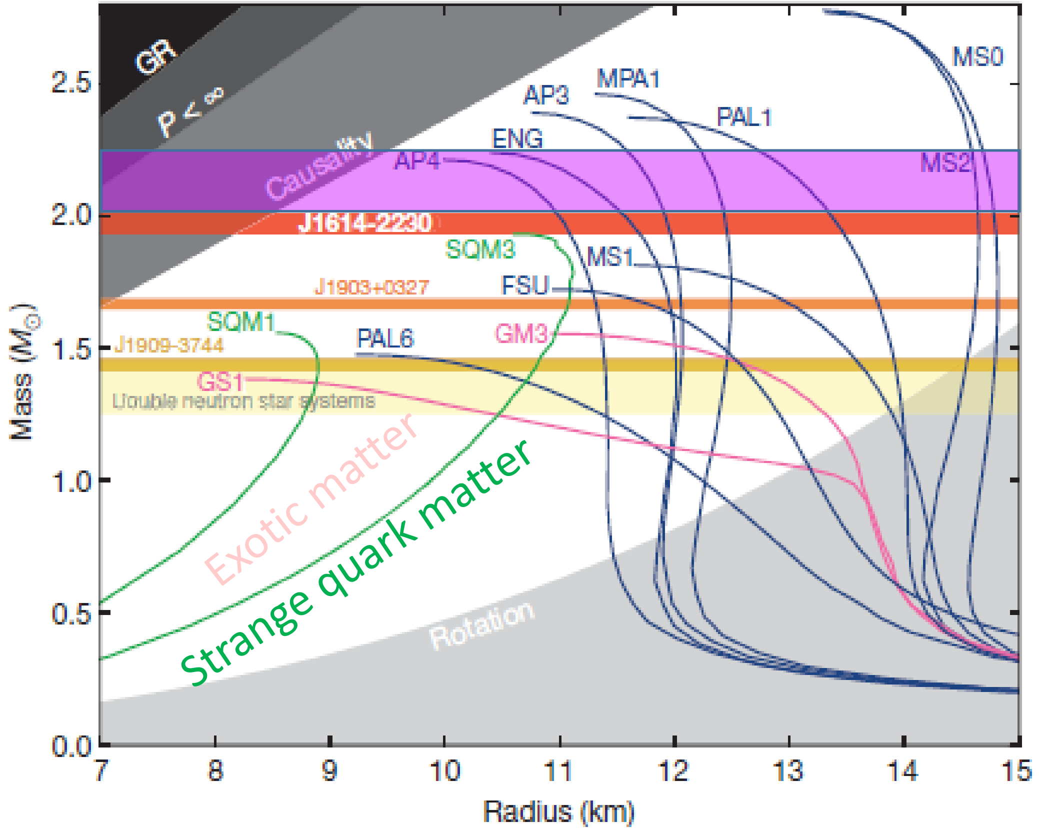

doi:10.1038/nature09466

- $M(R)$ is obtained as a solution of the TOV – equations with an only input – **EoS**.

$$\frac{dP}{dr} = -\frac{G\rho m}{r^2}\left(1+\frac{P}{\rho c^2}\right)\left(1+\frac{4\pi P r^3}{mc^2}\right)\left(1-\frac{2Gm}{c^2 r}\right)^{-1}$$

$$\frac{dm}{dr} = 4\pi r^2 \rho$$

Application: $M(R)$ of a β^- stable star

- One of the strongest constraints that we have is the maximum mass that the model predicts.

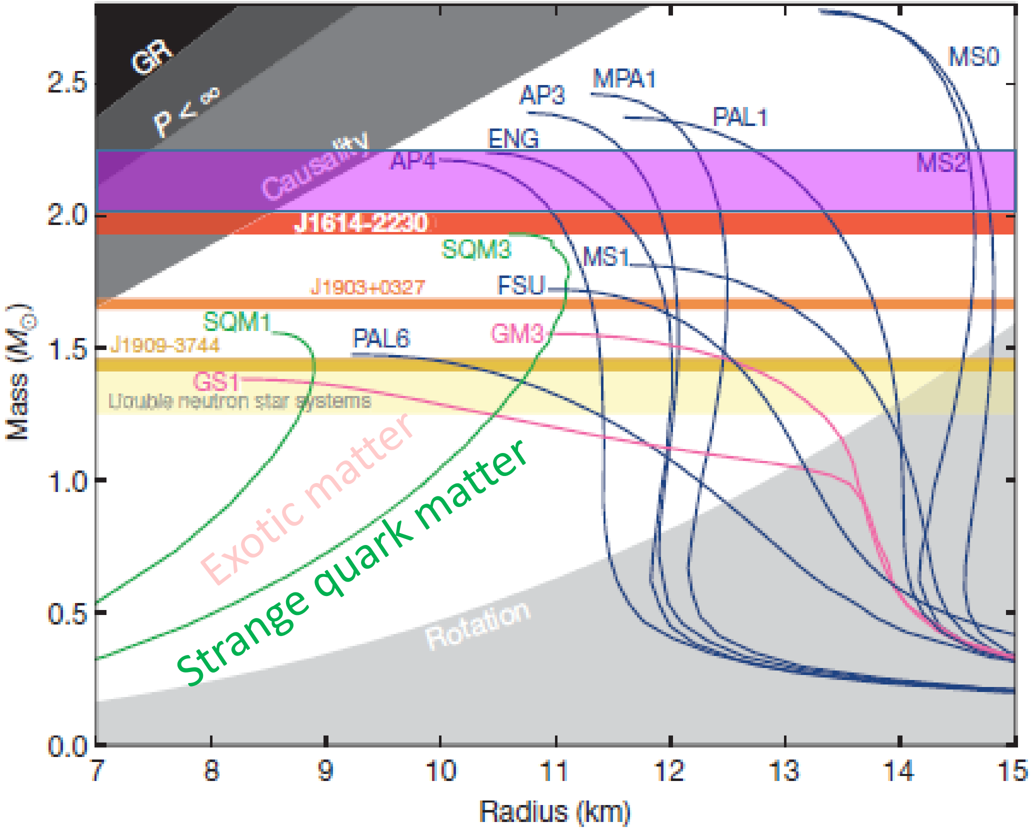

doi:10.1038/nature09466

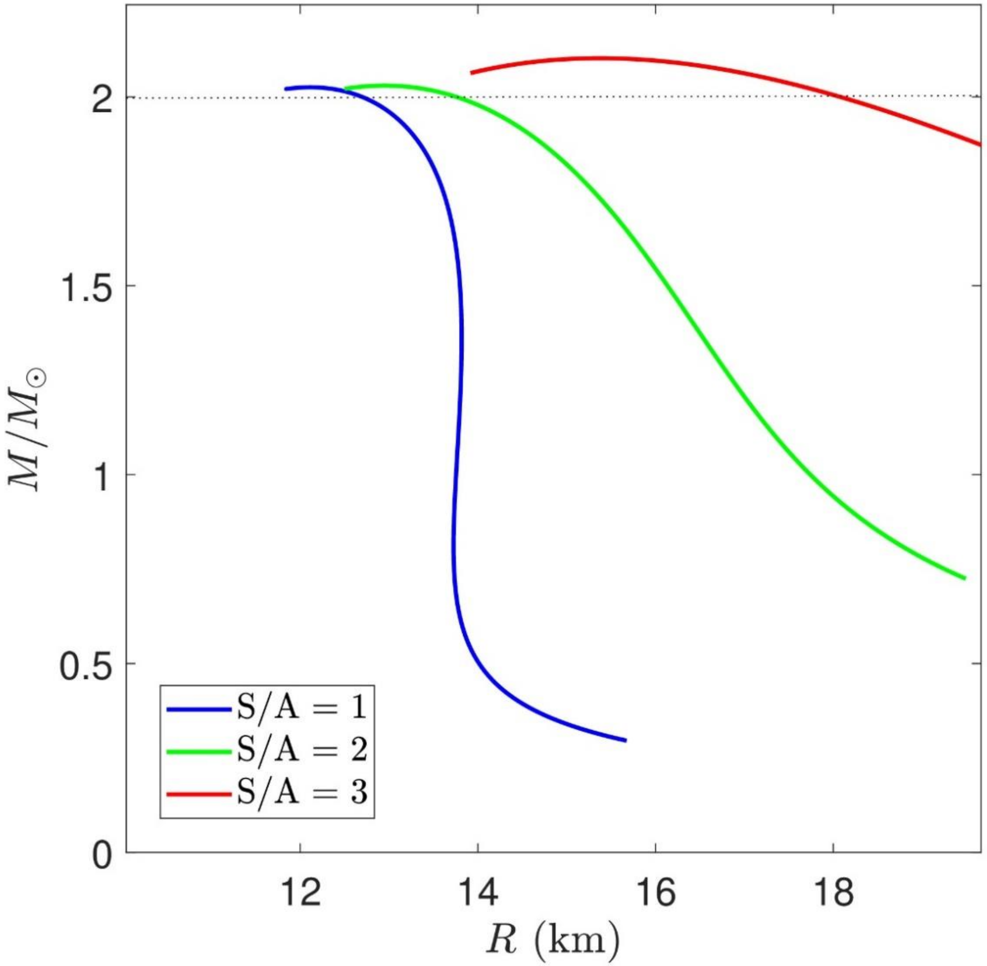

Application: $M(R)$ of a β^- stable star

- One of the strongest constraints that we have is the maximum mass that the model predicts.

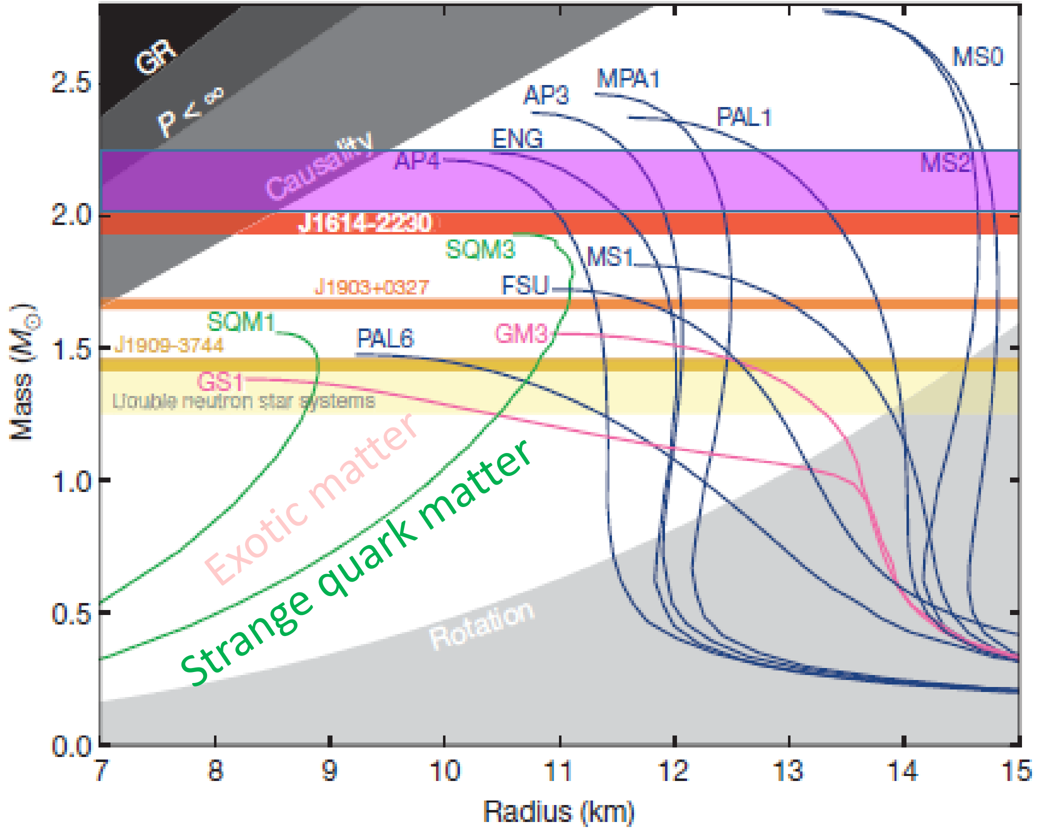

doi:10.1038/nature09466

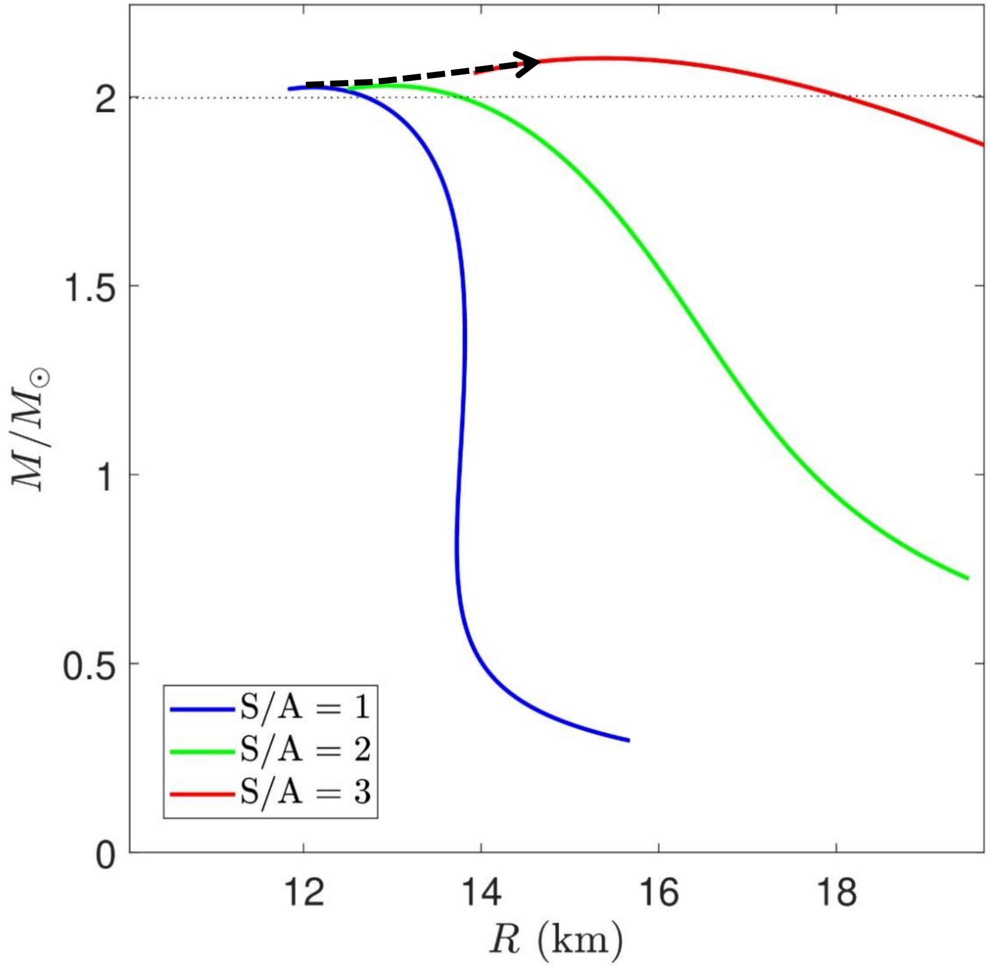

- M_{max} increases with S/A.
- The radius significantly shifts toward higher values with an increase of S/A.

Summary

- We extended the **FSU2H** hyperonic model to finite temperature, constructing the new so-called **FSU2H*** model, in order to be used in early stages of NS evolution and in NS mergers.

- The baryonic EoS is properly tabulated, making it useful for relativistic simulations.

- All baryons of the baryon octet can be found in the core of the star and in certain regimes their contribution can be significant.

- $P(\rho_B)$ and $\epsilon(\rho_B)$ are sensitive to the temperature and charge fraction of star matter at which the star is considered.

- To show the usefulness of the EoS we obtained the $M(R)$ relation for beta stable stars at constant S/A.

Thank you for your attention

Supported by:

Hristijan Kochankovski
Laura Tolos
Àngels Ramos

HYP2022
Prague, Czech Republic

30.06.2022

Back up slides

Supported by:

Hristijan Kochankovski
Laura Tolos
Àngels Ramos

HYP2022
Prague, Czech Republic

30.06.2022

RMF model extended I

$$(i\gamma_\mu\partial^\mu - m_b^* - g_{\omega b}\gamma_0\omega^0 - g_{\phi b}\gamma_0\phi^0 - g_{\rho b}I_{3b}\gamma_0\rho_3^0)\Psi_b = 0,$$
$$(i\gamma_\mu\,\partial^\mu - q_l\,\gamma_\mu\,A^\mu - m_l)\,\psi_l = 0,$$

Baryon’s and lepton’s equations of motions

$$m_\sigma^2\bar{\sigma} + \frac{\kappa}{2}g_{\sigma b}^3\bar{\sigma}^2 + \frac{\lambda}{3!}g_{\sigma b}^4\bar{\sigma}^3 = \sum_b g_{\sigma b}\rho_b^s,$$
$$m_{\sigma^*}^2\bar{\sigma}^* = \sum_{b^*} g_{\sigma b^*}\rho_b^s$$
$$m_\omega^2\bar{\omega} + \frac{\zeta}{3!}g_{\omega b}^4\bar{\omega}^3 + 2\Lambda_\omega g_{\rho,b}^2 g_{\omega,b}^2\bar{\omega}\bar{\rho}^2 = \sum_b g_{\omega b}\rho_b,$$
$$m_\rho^2\bar{\rho} + 2\Lambda_\omega g_{\rho,b}^2 g_{\omega,b}^2\bar{\omega}^2\bar{\rho} = \sum_b\; g_{\rho b}I_{3b}\rho_b,$$
$$m_\phi^2\bar{\phi} = \sum_b g_{\phi b}\rho_b,$$

Meson’s equation of motion in RMF approximation

$$\rho_b = <\bar{\Psi}_b\gamma^0\Psi_b> = \frac{\gamma_b}{2\pi^2}\int_0^\infty dk\,k^2\,f_b(k,T),$$
$$\rho_b^s = <\bar{\Psi}_b\Psi_b> = \frac{\gamma_b}{2\pi^2}\int_0^\infty dk\,k^2\,\frac{m_b^*}{\sqrt{k^2+{m_b}^{*2}}}f_b(T,k)$$

Scalar and baryonic density

$$f_b(k,T) = \left[1 + exp\left(\frac{\sqrt{k^2+m_b^{*2}} - \mu_b^*}{T}\right)\right]^{-1}$$

Fermi – dirac distribution

$$\mu_b^* = \mu_b - g_{b\omega}\bar{\omega} - g_{b\rho}\bar{\rho} - g_{b\phi}\bar{\phi}.$$
$$m_b^* = m_b - g_{\sigma b}\sigma - g_{\sigma^* b}\sigma^*,$$

Effective chemical potential and charge neutrality

RMF model extended II

$$\mu_{b^0} = \mu_n,$$
$$\mu_{b^-} = 2\mu_n - \mu_p,$$
$$\mu_{b^+} = \mu_p,$$
$$\mu_n - \mu_p = \mu_e - \mu_{\nu_e},$$
$$\mu_e = \mu_\mu + \mu_{\nu_e} - \mu_{\bar{\nu}_\mu},$$

β equilibrium

$$\rho_B = \sum_b \rho_b,$$
$$Y_l \cdot \rho_B = \rho_l + \rho_{\nu_l}$$

Conservation of baryon and lepton numbers

$$T_{\mu\nu} = \frac{\partial \mathcal{L}}{\partial(\partial_\mu \Phi_\alpha)} \partial^\mu \Phi_\alpha - \eta_{\mu\nu}\mathcal{L},$$

Energy-momentum tensor

$$\begin{aligned}
\epsilon &= < T_{00} > \\
&= \frac{1}{2\pi^2}\sum_b \gamma_b \int_0^\infty dk k^2 \sqrt{k^2 + m_b^{*2}} f_b(k,T) \\
&+ \frac{1}{2\pi^2}\sum_l \gamma_l \int_0^\infty dk k^2 \sqrt{k^2 + m_l^2} f_l(k,T) \\
&+ \frac{1}{2}(m_\omega^2 \bar{\omega}^2 + m_\rho^2 \bar{\rho}^2 + m_\phi^2 \bar{\phi}^2 + m_\sigma^2 \bar{\sigma}^2 + m_{\sigma^*}^2 \bar{\sigma}^{*2}) \\
&+ \frac{\kappa}{3!}(g_\sigma \bar{\sigma})^3 + \frac{\lambda}{4!}(g_\sigma \bar{\sigma})^4 + \frac{\zeta}{8}(g_\omega \bar{\omega})^4 + 3\Lambda_\omega (g_\rho g_\omega \bar{\rho}\bar{\omega})^2, \\
P &= \frac{1}{3} < T_{jj} > \\
&= \frac{1}{6\pi^2}\sum_b \gamma_b \int_0^\infty dk \frac{k^4}{\sqrt{k^2 + m_b^{*2}}} f_b(k,T) \\
&+ \frac{1}{6\pi^2}\sum_l \gamma_l \int_0^\infty dk \frac{k^4}{\sqrt{k^2 + m_l^2}} f_l(k,T) \\
&+ \frac{1}{2}(m_\omega^2 \bar{\omega}^2 + m_\rho^2 \bar{\rho}^2 + m_\phi^2 \bar{\phi}^2 - m_\sigma^2 \bar{\sigma}^2 - m_{\sigma^*}^2 \bar{\sigma}^{*2}) \\
&- \frac{\kappa}{3!}(g_\sigma \bar{\sigma})^3 - \frac{\lambda}{4!}(g_\sigma \bar{\sigma})^4 + \frac{1}{24}\zeta(g_\omega \bar{\omega})^4 + \Lambda_\omega (g_\rho g_\omega \bar{\rho}\bar{\omega})^2,
\end{aligned}$$

$$s = \frac{1}{T}\left(\epsilon + P - \sum_i \mu_i \rho_i\right)$$
$$f = \sum_i \mu_i \rho_i - P.$$

Thermodynamic quantities

Temperature profiles and tidal deformability

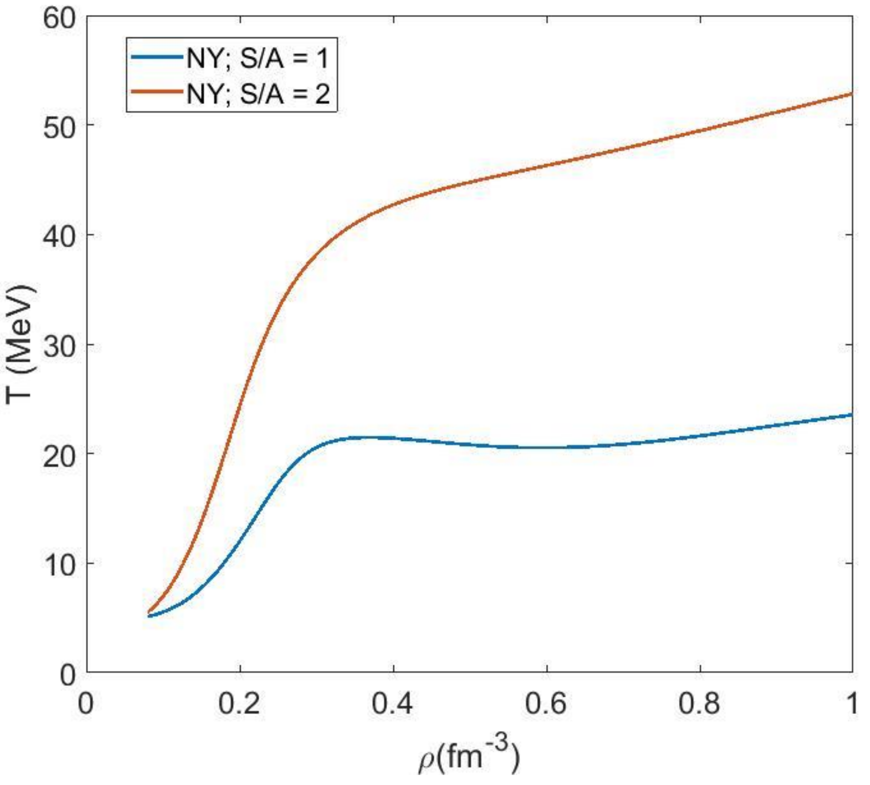

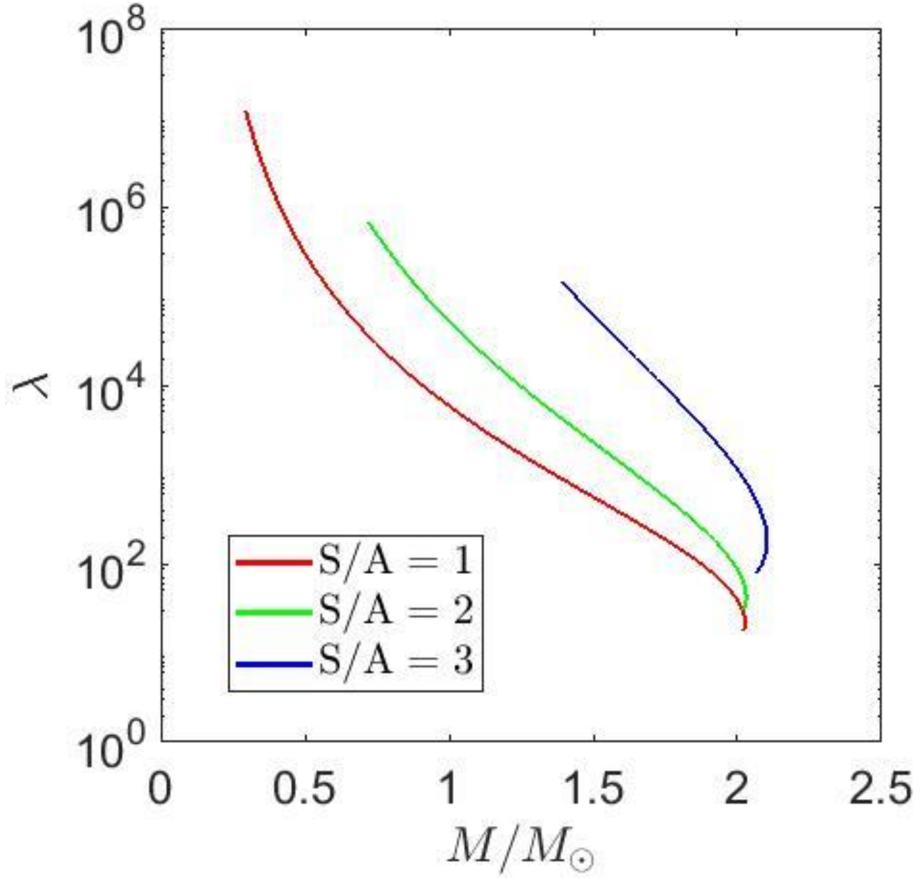

Why FSU2H* model? I

PASA, 34, e065 (2017)

$\boldsymbol{\rho_0}$ (fm^{-3})	**E/A** (MeV)	K (MeV)	m_N^*/m_N (ρ_0)	$E_{sym}(\rho_0)$ (MeV)	L (MeV)	K_{sym} (MeV)
0.1505	-16.28	238.0	0.593	30.5	44.5	86.4

Consistent with the majority of the calculations, variety of nuclear data from terrestrial experiments, astrophysical observations…

Why FSU2H* model? I

m_σ (MeV)	m_ω (MeV)	m_ρ (MeV)	m_{σ^*} (MeV)	m_ϕ (MeV)	$g^2_{\sigma N}$	$g^2_{\omega N}$	$g^2_{\rho N}$	κ (MeV)	λ	ζ	Λ_ω
497.479	782.500	763.000	980.000	1020.000	102.72	169.53	197.27	4.00014	-0.0133	0.008	0.045

Values of parameters in the model

PASA, 34, e065 (2017)

$\boldsymbol{\rho_0}$ (fm^{-3})	**E/A** (MeV)	K (MeV)	m_N^*/m_N (ρ_0)	$E_{sym}(\rho_0)$ (MeV)	L (MeV)	K_{sym} (MeV)
0.1505	-16.28	238.0	0.593	30.5	44.5	86.4

Consistent with the majority of the calculations, variety of nuclear data from terrestrial experiments, astrophysical observations…

Why FSU2H* model? I

m_σ (MeV)	m_ω (MeV)	m_ρ (MeV)	m_{σ^*} (MeV)	m_ϕ (MeV)	$g^2_{\sigma N}$	$g^2_{\omega N}$	$g^2_{\rho N}$	κ (MeV)	λ	ζ	Λ_ω
497.479	782.500	763.000	980.000	1020.000	102.72	169.53	197.27	4.00014	-0.0133	0.008	0.045

Values of parameters in the model

PASA, 34, e065 (2017)

- The properties of the model at T = 0 are listed in the table

$\boldsymbol{\rho_0}$ (fm^{-3})	**E/A** (MeV)	K (MeV)	m^*_N/m_N (ρ_0)	$E_{sym}(\rho_0)$ (MeV)	L (MeV)	K_{sym} (MeV)
0.1505	-16.28	238.0	0.593	30.5	44.5	86.4

Consistent with the majority of the calculations, variety of nuclear data from terrestrial experiments, astrophysical observations…

Why FSU2H* model? I

m_σ (MeV)	m_ω (MeV)	m_ρ (MeV)	m_{σ^*} (MeV)	m_ϕ (MeV)	$g^2_{\sigma N}$	$g^2_{\omega N}$	$g^2_{\rho N}$	κ (MeV)	λ	ζ	Λ_ω
497.479	782.500	763.000	980.000	1020.000	102.72	169.53	197.27	4.00014	-0.0133	0.008	0.045

Values of parameters in the model

PASA, 34, e065 (2017)

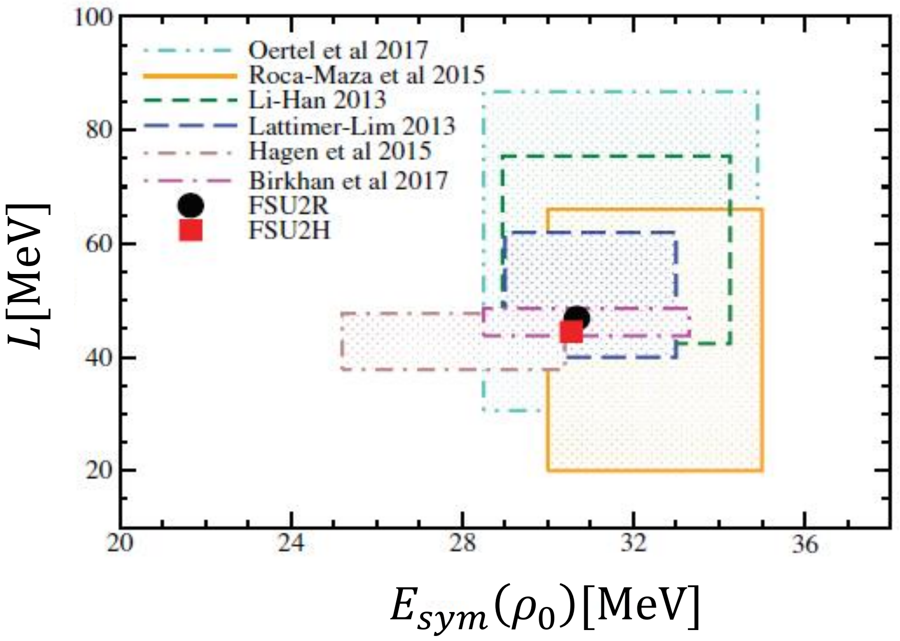

Low density region constrains

- The properties of the model at T = 0 are listed in the table

ρ_0 (fm^{-3})	E/A (MeV)	K (MeV)	m^*_N/m_N (ρ_0)	$E_{sym}(\rho_0)$ (MeV)	L (MeV)	K_{sym} (MeV)
0.1505	-16.28	238.0	0.593	30.5	44.5	86.4

Consistent with the majority of the calculations, variety of nuclear data from terrestrial experiments, astrophysical observations…

Why FSU2H* model? II

Why FSU2H* model? II

Values of the parameters in the model related to hyperons

Y	$R_{\sigma Y}$	$R_{\omega Y}$	$R_{\rho Y}$	$R_{\sigma^* Y}$	$R_{\phi Y}$
Λ	0.6613	2/3	0	0.2812	$-\sqrt{2}/3$
Σ	0.4673	2/3	2	0.2812	$-\sqrt{2}/3$
Ξ	0.3305	1/3	1	0.5624	$-2\sqrt{2}/3$

$$R_{iY} = \frac{g_{iY}}{g_{iN}};\, i = (\sigma, \omega, \rho);\ R_{\sigma^* Y} = \frac{g_{\sigma^* Y}}{g_{\sigma Y}}; R_{\phi Y} = \frac{g_{\phi Y}}{g_{\omega N}}$$

Flavour SU(3) symmetry, the vector dominance model, and ideal mixing for the physical ω and ρ field

Why FSU2H* model? II

Values of the parameters in the model related to hyperons

Y	$R_{\sigma Y}$	$R_{\omega Y}$	$R_{\rho Y}$	$R_{\sigma^* Y}$	$R_{\phi Y}$
Λ	0.6613	2/3	0	0.2812	$-\sqrt{2}/3$
Σ	0.4673	2/3	2	0.2812	$-\sqrt{2}/3$
Ξ	0.3305	1/3	1	0.5624	$-2\sqrt{2}/3$

$$R_{iY} = \frac{g_{iY}}{g_{iN}};\, i = (\sigma, \omega, \rho);\ R_{\sigma^* Y} = \frac{g_{\sigma^* Y}}{g_{\sigma Y}}; R_{\phi Y} = \frac{g_{\phi Y}}{g_{\omega N}}$$

Flavour SU(3) symmetry, the vector dominance model, and ideal mixing for the physical ω and ρ field

Potential felt by a hyperon *i* in *j*-particle matter is given by

$$U_i^{(j)}(\rho_j) =$$
$$= -g_{\sigma i}\bar{\sigma}^{(j)} - g_{\sigma i}\bar{\sigma}^{*(j)} + g_{\omega i}\bar{\omega}^{(j)} + g_{\rho i} I_{3i}\bar{\rho}^{(j)} + g_{\phi i}\bar{\phi}^{(j)}$$

Why FSU2H* model? II

Values of the parameters in the model related to hyperons

Y	$R_{\sigma Y}$	$R_{\omega Y}$	$R_{\rho Y}$	$R_{\sigma^* Y}$	$R_{\phi Y}$
Λ	0.6613	2/3	0	0.2812	$-\sqrt{2}/3$
Σ	0.4673	2/3	2	0.2812	$-\sqrt{2}/3$
Ξ	0.3305	1/3	1	0.5624	$-2\sqrt{2}/3$

$$R_{iY} = \frac{g_{iY}}{g_{iN}};\, i = (\sigma, \omega, \rho);\ R_{\sigma^* Y} = \frac{g_{\sigma^* Y}}{g_{\sigma Y}}; R_{\phi Y} = \frac{g_{\phi Y}}{g_{\omega N}}$$

Flavour SU(3) symmetry, the vector dominance model, and ideal mixing for the physical ω and ρ field

Potential felt by a hyperon *i* in *j*-particle matter is given by

$$U_i^{(j)}(\rho_j) =$$
$$= -g_{\sigma i}\bar{\sigma}^{(j)} - g_{\sigma i}\bar{\sigma}^{*(j)} + g_{\omega i}\bar{\omega}^{(j)} + g_{\rho i} I_{3i}\bar{\rho}^{(j)} + g_{\phi i}\bar{\phi}^{(j)}$$

$$U_\Lambda^{(N)}(\rho_0) = -28 \text{ MeV};$$

$$U_\Sigma^{(N)}(\rho_0) = 30 \text{ MeV};$$

$$U_\Xi^{(N)}(\rho_0) = -22 \text{ MeV};$$

Hyperon potentials in SNM

Why FSU2H* model? III

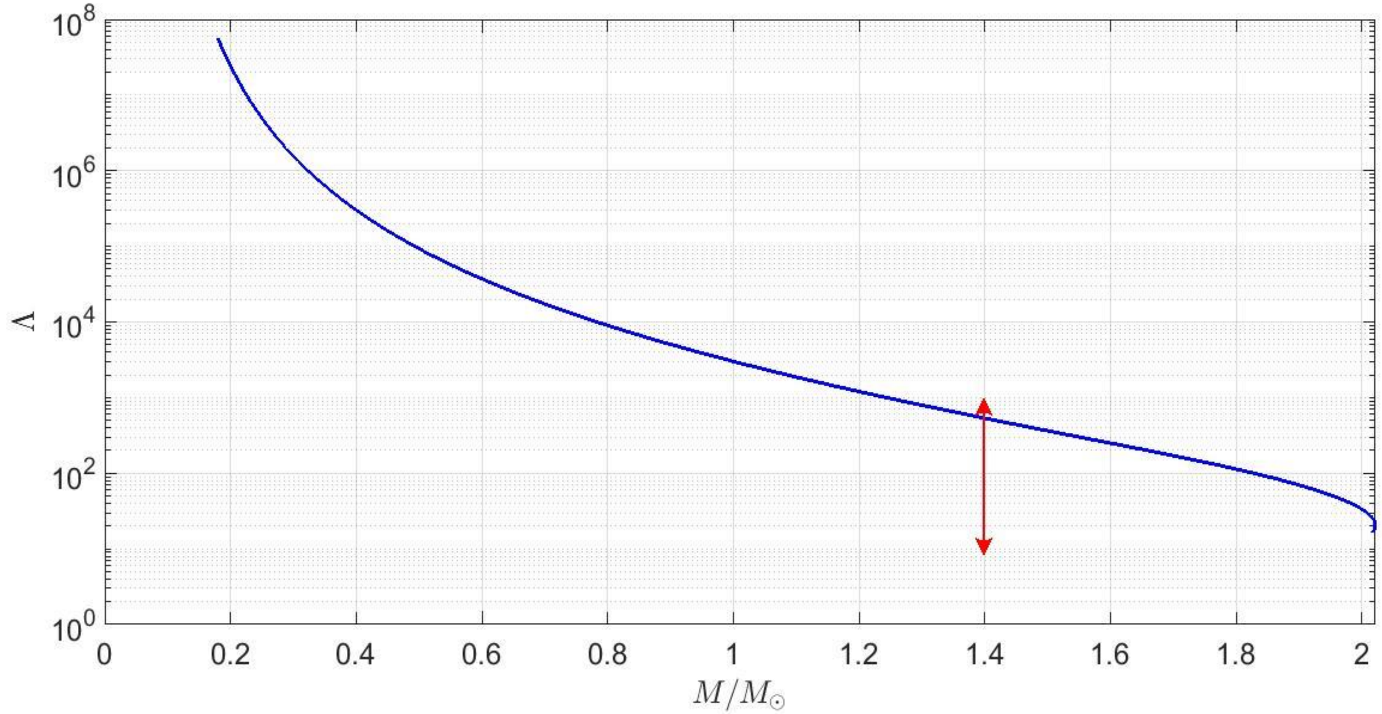

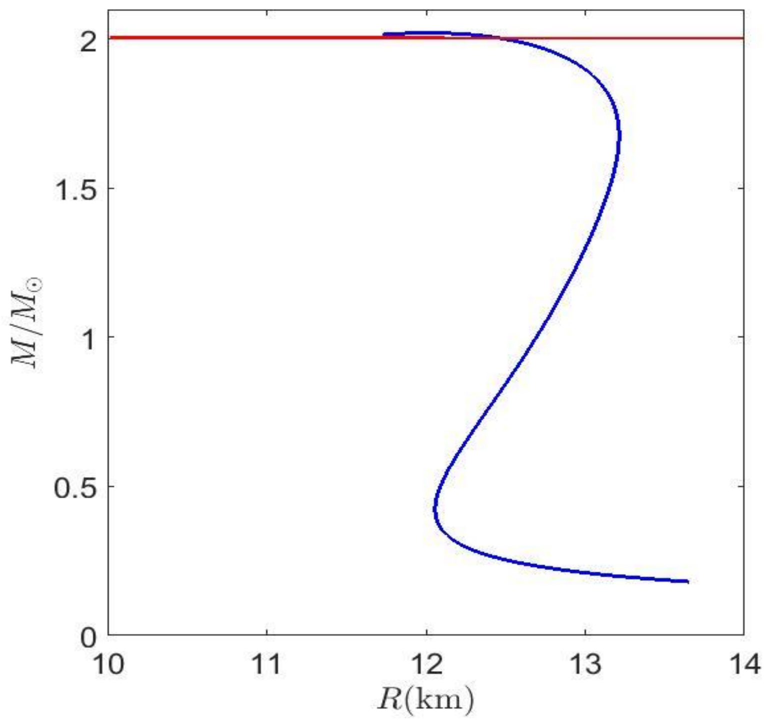

Intermediate and high density regions constrains

$M_{\mathbf{max}}$ $(M_\odot)$	$R(M_{\mathbf{max}})$ (km)	$R(1.4M_\odot)$ (km)	$\mathbf{\Lambda}(1.4M_\odot)$
2.03	12.02	13.08	526.3

In agreement with:

- $\boldsymbol{M_{\max} > 2M_\odot}$
- **70 < $\mathbf{\Lambda(1.4M_\odot)}$ < 580**
- **10.5 km < $\mathbf{R(1.4M_\odot)}$ < 13.3 km**

Speed of sound (T = 0)

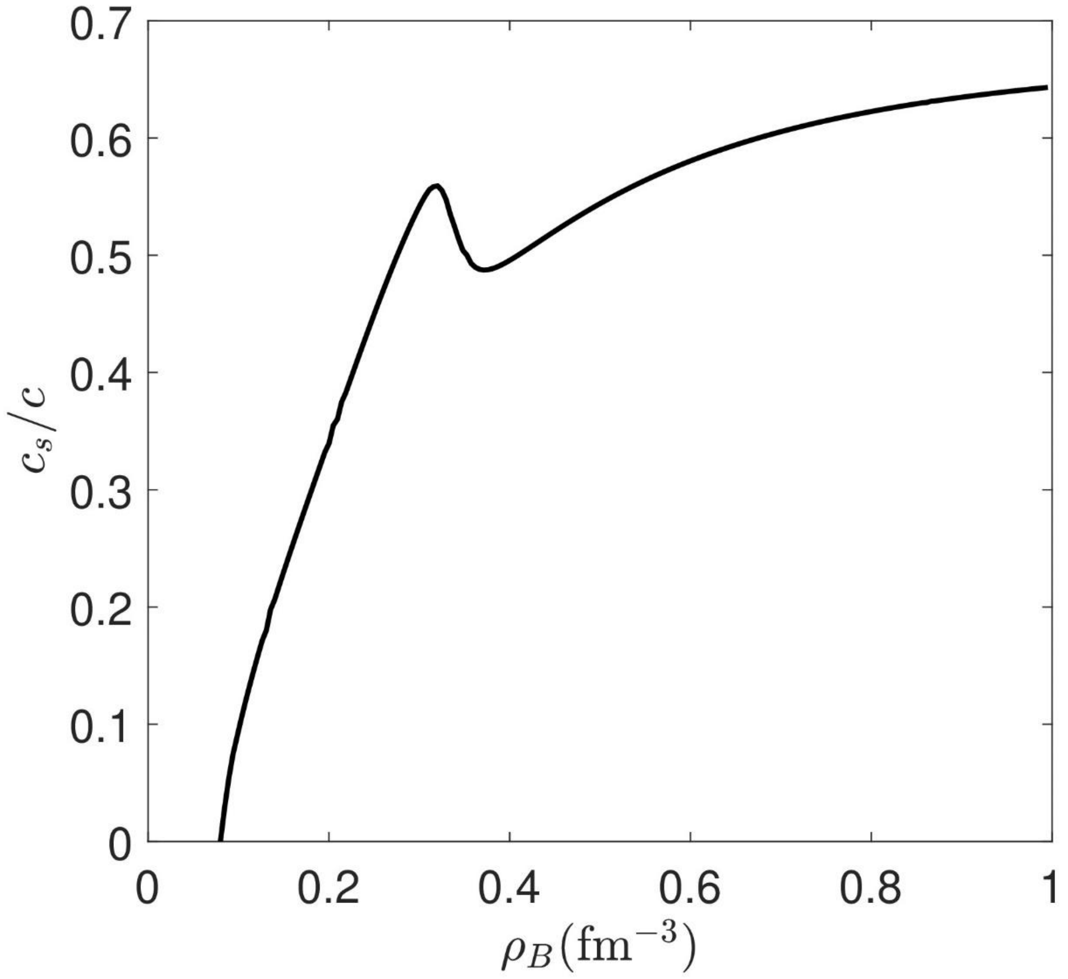

$$\frac{c_s}{c} = \sqrt{\frac{dp}{d\epsilon}}$$